NASA CONTRACTOR REPORT

NASA CR-1329

NASA CR-1329

HELIOGYRO SOLAR SAILER SUMMARY REPORT

by Richard H. MacNeal, John P. Hedgepeth, and Hans U. Schuerch

Prepared by
ASTRO RESEARCH CORPORATION
Santa Barbara, Calif.
for

NATIONAL AERONAUTICS AND SPACE ADMINISTRATION • WASHINGTON, D. C. • JUNE 1969

NASA CR-1329

HELIOGYRO SOLAR SAILER

SUMMARY REPORT

By Richard H. MacNeal, John M. Hedgepeth,
and Hans U. Schuerch

Issued by Originator as Report No. ARC-R-297

Prepared under Contract No. NAS 7-427 by
ASTRO RESEARCH CORPORATION
Santa Barbara, Calif.

for

NATIONAL AERONAUTICS AND SPACE ADMINISTRATION

For sale by the Clearinghouse for Federal Scientific and Technical Information
Springfield, Virginia 22151 – CFSTI price $3.00

FOREWORD

Since November 1966, Astro Research Corporation has been conducting studies of the feasibility of a solar-sail vehicle that employs long, narrow blades made from thin films. This work has been performed under Contract NAS7-427 for National Aeronautics and Space Administration.

SUMMARY

Studies have been performed on the feasibility of a large solar-sail vehicle using long, narrow blades and operating in the manner of a helicopter rotor. This vehicle, the Heliogyro, is superior to other propulsion and attitude-control systems for many missions requiring large total impulse and long flight times.

Secondary uses of the extremely large surface areas inherent in the solar-sail concept include atmospheric braking and micrometeoroid sampling.

A conceptual configuration has been evolved in which the thin aluminized film blades are unrolled from spools during deployment. Centrifugal forces are used for stiffening the long, narrow solar sails.

Control of the attitude of the sail with respect to the solar rays is accomplished by pivoting the deployment spools and thus rotating the long blades about their lengthwise axes. Combinations of collective and cyclic blade pitch can provide all of the required control responses.

Results of the various theoretical analyses which have led to this Heliogyro solar-sailer concept are summarized. Evaluations of a number of missions are presented. The desirability of an experimental program to develop technology and establish feasibility is indicated.

CONTENTS

LIST OF ILLUSTRATIONS

List of Illustrations (continued)

INTRODUCTION

The presence of man and man-made devices in space is motivated to a great extent by the opportunity to utilize "locally accessible resources" in the form of materials, energy, impulse, or information.

The value of solar radiation as a locally available source of power for space missions has long been recognized. For instance, the concept of converting solar energy to electrical power and subsequent use of this power to produce thrust has received a great deal of attention and has given rise to the development of a solar-cell-powered electric-propulsion technology.

Useful thrust from solar photons can also be obtained directly. Hence the use of radiation pressure to provide propulsion for interplanetary space flight has been an attractive possibility for a number of years (Refs. 1-6). Since "solar sailing" requires no expendable propellant, it can provide thrust for an indefinite time and thus impart the velocity increments required for a series of separate space missions. The available pressures, however, are extremely low (approximately one newton per 100,000 square meters in the vicinity of the earth) so that very large sail areas are required to produce reasonable forces.

Radiation pressure is produced when light is incident upon a solid, absorbing, or reflecting surface. In the case of complete reflection from smooth surfaces, the pressure is normal to the surface and is proportional to the square of the cosine of the incident angle. In this respect, photon pressure is similar to aerodynamic pressure developed in free molecular flow. The analogy between photon pressure and aerodynamic pressure leads to the characterization of the solar sail as an interplanetary flying machine (Ref. 7). Force in the direction of orbital motion is obtained by inclining the surface with respect to the direction of the illumination.

The Heliogyro solar sailer is a new structural design concept for constructing, deploying, and controlling the required large sail area. Although sufficiently lightweight materials are available for making sails, practical techniques have not previously been available for unfurling and rigidizing such large areas.

The mechanics of the solar sail in orbit around the sun have been described in a number of papers (Refs. 2, 4, 6, and 8). The parameter most commonly used to characterize the performance of a solar sail is the lightness number, λ . It is defined as the ratio of the radiation force on the sail to the attractive force of the sun's gravitational field

$$\lambda = \frac{p_o A}{F_G}$$

where p_o is the radiation pressure for normal incidence, A is the sail area, and F_G is the gravitational force of the sun exerted upon the spacecraft. Since both p_o and F_G vary inversely as the square of the distance from the sun, the lightness number is independent of position within the solar system.

The lightness number, λ_s , of the sail and supporting structure is also related to the familiar propulsion-system specific impulse, I_{sp} , (i.e., the impulse per unit of propulsion-system weight). Figure 1* shows the relative performance ranges for "state-of-art" and "advanced" versions of solar sails, solar-energy-powered electrical propulsion and chemical propulsion systems.

The material most commonly considered for the solar sail is a very thin sheet of plastic with aluminized surfaces. The aluminum coating is a good reflector and also protects the plastic film from damage due to ultraviolet rays. Mylar films that are one-quarter of a thousandth of an inch thick are commercially produced in large quantities. The manufacture of films that are one-twentieth of a thousandth of an inch thick is considered to be feasible. Figure 2 shows that these films will permit lightness numbers of 0.3 to be attained with a reasonable percentage of payload weight on the Heliogyro solar sailer.

Solar sails are not useful as propulsive devices for low earth orbits. Aerodynamic effects overcome the solar pressure

---

* Excerpted from supporting studies performed by R.H. MacNeal, MacNeal-Schwendler Corporation Report MSR-13, October 1968.

for altitudes of less than about 500 miles above the earth. The large drag areas of the sails may, however, be employed for aerodynamic braking at extremely high altitudes. This constitutes one of several secondary uses of the large deployed surface areas inherent in the solar-sail concept.

HELIOGYRO CONCEPT

Structural Design

The critical requirements for structural design are: 1) to maximize the ratio of reflecting surface area to structural weight, so as to produce a large lightness number, 2) to package the large surfaces within the volume of a booster payload in a manner that will permit reliable deployment, and 3) to provide a means for changing the direction of the resultant radiation force, thus permitting maneuvers of the vehicle within the sun's gravitational field.

The deployed surface area and total vehicle weight are determined by performance requirements and the properties of available materials. The size of the packaged Heliogyro is determined by the payload dimensions of existing booster rockets. Within these constraints, design tradeoff studies can be performed on the selection of shape of sail, on the method for deploying and rigidizing it, and on the technique for controlling the direction of the resultant force.

Consideration is given to a number of sail shapes and rigidization techniques in Reference 7. It is concluded that long, rectangular strips, stowed by winding on spools, represent the best compromise for sail shape. Centrifugal force is selected as the preferred method for rigidizing the long, narrow sails on the basis of minimum weight and minimum complexity.

The orientation of solar sails could be changed by shading of one reflecting surface by another, or by shifting of the center of gravity of the payload. In the case of long, narrow blades, the simplest method of orientation is to pitch the blades about their lengthwise axes. The resultant magnitudes and directions of the radiation forces on the blades can then be controlled by a centrally located mechanism.

In summary, the structural design concept developed for the Heliogyro solar sailer employs long, narrow blades which are rigidized by centrifugal force and which are rotated about their lengthwise axes to provide spin torque and precessional moments. The choice of long, narrow blades is based primarily on booster-rocket volume constraints. Centrifugal force was selected to

stiffen the long, narrow blades because no other technique was found to be suitable for the extreme lengths required. Blade pitch was selected for the control system because of its mechanical simplicity and because it can provide all of the desired control responses.

To illustrate the Heliogyro design concept and to explore the practicability of a small experimental flight model, a preliminary design was made of a two-blade configuration. As shown in Figures 3 and 4, it resembles a helicopter rotor in that it uses long, narrow blades which are stiffened by centrifugal forces and are controlled by pitch mechanisms. Technical characteristics of this experimental model are summarized in Table I.

TABLE I. TECHNICAL CHARACTERISTICS OF EXPERIMENTAL TWO-BLADE MODEL HELIOGYRO

Gross Weight	550 lb
Non-Sail Weight	200 lb
Lightness Number	0.1
Blade Material	1/4-mil Mylar with 1500 Å of aluminum coating, each side
Blade Area	180 000 ft^2
Blade Tip Radius	18 600 ft
Blade Chord	4.84 ft
Rotational Period	6 minutes
Blade Root Stress	1000 psi
Blade Tip Speed	326 ft/sec
Root Coning Angle	0.000425 radian
Polar Moment of Inertia	1.28×10^9 lb-sec^2-ft

The deployment sequence for the two-blade model is shown in Figure 5. A small angular velocity (about 2 revolutions per second) is produced by rocket motors in order to develop initial tension in the blades. The blades are then unrolled about 300 feet and pitched

collectively. Solar radiation spins the blades as shown. The blades are then gradually unrolled as the angular momentum increases.

Blade Configuration

The size, shape, and general performance characteristics of the Heliogyro may be determined without a detailed evaluation of the design of the long, flexible blades. In order to investigate maneuvering capability, rotational speed, deployment sequence, and stress distribution, however, the blade configuration must be analyzed. A detailed analysis of the mechanics of a thin, flexible blade subjected to centrifugal force and photon pressure is presented in Reference 7. A summary of the characteristics of these blades is treated in this section.

Practical materials for solar-sail construction to achieve suitable lightness numbers have received considerable attention. It has been shown (Ref. 2) that the maximum possible lightness number resulting as a balance between opacity and film thickness is about 5.0. Metal films about 500 Angstroms in thickness would be required to achieve this upper limit. Aluminum sheets approximately 3000 Angstroms thick, deposited on films which sublime in space have been proposed (Ref. 1), and a limited amount of experimental work has been performed. A more practical candidate material for solar sails is a Mylar sheet covered on both sides by a deposited aluminum film. Mylar is the lightest continuous film currently available in large production quantities. Samples of one-twentieth mil Mylar have been produced, and quarter-mil aluminized Mylar sheets are available in rolls 56 inches wide at a cost of less than 2 cents per square foot.

In Figure 2 the relationship is shown between lightness number, payload weight fraction, and sheet thickness for a Mylar sheet coated with an aluminized film 3000 Angstroms thick. For a given thickness of Mylar, the selection of the combination of lightness number and payload weight fraction is made on the basis of performance requirements. For example, for tenth-mil Mylar, a heavy payload can be carried with a lightness number of 0.1, or a light payload can be carried with a lightness number of 0.4. Also, for standard quarter-mil Mylar, a practical lightness number is approximately 0.1.

Long exposure of solar sails to the space environment has been considered (Ref. 5). Hazards include temperature extremes, micrometeoroids, proton bombardment, and ultraviolet radiation.

Temperature does not appear to be a critical problem for the materials and stress levels being considered for the Heliogyro unless missions are considered that involve trajectories in the close vicinity of the sun. Solar protons will cause sputtering of the aluminum coating; recent data, however, (Ref. 9) has shown the erosion rate to be of the order of one Angstrom per year. Micrometeoroids will pierce the sails and may cause some loss in surface reflectivity, but the proportion of the surface area punctured in one year is of the order of 10^{-5}. At the low stress levels planned, this will not affect the structural integrity. Ultraviolet radiation will cause deterioration of exposed Mylar, but the aluminum coating effectively eliminates this source of damage. The general conclusion is that, for most applications, no unsurmountable problems of material deterioration due to the space environment have been discovered.

Three types of blade deformations are analyzed in Reference 7. Vertical, or flapwise deflections include coning which affects thrust and may introduce precessional torques. Inplane or chordwise deflections include bending camber or curling. The third deformation is twist or blade pitch. A coupling analysis of flapwise, chordwise, and twisting deflections has not been completed, but interesting conclusions have been drawn from analysis of each of the three modes separately.

Centrifugal force is the main stiffening agent for each of the three types of deformation. Bending stiffness is important only during the initial stages of deployment and is negligible for the extended blades.

The vertical deflection of the blades for the two-blade model vehicle is shown in Figure 6 for an assumed stress at the blade root of 1000 psi. The ordinate is the parameter $w/\beta_o R$ where w is the deflection normal to the blade, β_o is the coning angle at the blade root, and R is the blade tip radius. The root coning angle shown for this example is 0.000425 radian, and the mean coning angle selected at the 75 percent chord point is 0.00024 radian. The actual blade shape is shown; the maximum deflection from the mean coning angle line occurs at the tip and is 0.4 foot or about 12 percent of the blade chord.

Large coning angles are undesirable for three reasons. First, the thrust due to solar illumination parallel to the axis of rotation varies as $\cos^3\beta$. Second, if the direction of illumination is not parallel to the axis of rotation, coning produces a steady

precessional torque on the vehicle. Third, curvature produces mechanical coupling between chordwise deformation and blade twist.

A primary requirement of blade pitching deflection is that it be possible to twist the entire blade by imposing a constant twist angle at the blade root. In Figure 7 is shown the variation of pitch angle θ, along the span of the blade for two twist conditions. The upper curve is for a constant pitch angle, θ_o, at the blade root and shows that the pitch angle at the tip is equal to about 36 percent of the imposed root pitch angle. The lower curve shows the twist resulting from a chordwise offset of the center of pressure from the tension axis of the blade. The normalizing factor, θ_x, is

$$\theta_x = 12 \left(\frac{p_n}{\sigma_o}\right) \cdot \left(\frac{R}{c}\right)^2 \cdot \left(\frac{x_{cp} - x_t}{t}\right)$$

where p_n is the pressure component normal to the surface, σ_o is the spanwise stress at the root, c is the blade chord, t is the blade thickness, and $x_{cp}-x_t$ is the center-of-pressure offset. For the two-blade example, the pitch angle at the tip for a one-inch offset of the center of pressure is about 0.1 radian. Thus, it is necessary to accurately control the chordwise locations of the center of pressure and center of gravity in order to maintain blade trim.

The blade will tend to camber or curl about a spanwise axis due to differential expansion. The chordwise membrane stress is too small to prevent camber, but chordwise battens at 100-foot intervals would be adequate; the weight increase would be about one percent of the sail weight.

Chordwise deformation of a blade subjected to 30 degrees of pitch, and with blade twist as shown in Figure 7, has been computed. The net loading on the outboard portion of the blade causes the blade tip to lag behind the blade root. For the two-blade vehicle this chordwise deflection is about three feet.

Two operational characteristics of the Heliogyro that depend on the length of the blade are the rotational period and the centripetal acceleration at the blade tip. The rotational period is given by

$$T = \pi R \sqrt{\frac{\rho}{2\sigma_o}}$$

and the tip acceleration is given by

$$g_{tip} = \frac{2\sigma_o}{\rho R}$$

where ρ is the density of the blade material and σ_o is the stress at the blade root. These parameters are plotted in Figure 8 as a function of the blade radius, R.

For operation in near earth orbits, the rotational period should be small compared to the orbital period. The effect of perturbing forces due to gravity gradient become serious if these times become nearly equal. Assuming the orbital period to be 100 minutes, the rotational period should be less than 20 minutes. From Figure 8, the maximum blade radius is about 60 000 feet unless the root stress is increased above 1000 psi.

Centripetal acceleration can be used in manned vehicles to provide an artificial gravitational field. From Figure 8, for the 1000-psi root stress limit, a one-tenth g acceleration exists at a radius of about 35 000 feet.

Control Characteristics

The means by which control forces and control moments are exerted on the Heliogyro are shown in Figure 9. Figure 9(a) illustrates the use of cyclic pitch to produce a steady component of force in the plane of the rotor. Figure 9(b) shows a rolling moment produced by a combination of cyclic and collective pitch. Collective pitch also produces spin torque and reduces the component of force normal to the rotor plane.

A derivation of the equations for the forces and moments on a rotor due to solar illumination is presented in Reference 7. The coordinate geometry used in this derivation is shown in Figure 10. A summary of the control characteristics assuming ideal reflectivity is as follows:

Case 1: Steady flight with no coning ($\beta = \theta = 0$).

Lift: $L = p_o n_b \cdot Rc \cdot \sin\gamma \cdot \cos^2\gamma$

Drag: $D = p_o\ n_b\ Rc \cdot \cos^3\gamma$

where p_o is the total radiation pressure and n_b is the number of blades.

Case 2: Longitudinal moment due to coning in steady flight

$$M_y = \frac{1}{2} \cdot p_o\ n_b c \cdot \sin 2\gamma \int_o^R r \cdot \sin\beta \cdot dr$$

Case 3: Cyclic pitch required to achieve zero longitudinal moment in steady flight. β = constant; $\theta = a_1 \sin\psi$, where a_1 is small.

$$a_1 = \frac{-\sin 2\gamma \cdot \cos\beta}{\cos^2\beta \cdot \cos^2\gamma + \frac{1}{4} \cdot \sin^2\gamma}$$

Case 4: Combined cyclic and collective pitch required to achieve zero longitudinal moment in steady flight, β = constant; $\theta = \theta_o + b_1 \cdot \cos\psi$ where θ_o and b_1 are small and constant along the span.

$$\theta_o \cdot b_1 = \frac{-\sin\beta \cdot \sin 2\gamma}{3 \cdot \cos^2\gamma - \frac{1}{2} \cdot \sin^2\gamma}$$

Case 5: Longitudinal control moment for no coning; $\beta = 0$, $\theta = \theta_o + b_1 \cos\psi$, where b_1 is small and constant along the span

$$M_y = \frac{3}{2} \cdot p_o\ b_1\ n_b\ c \int_o^R \sin\theta_o \cdot \cos^2\theta_o \left\{ \cos^2\gamma - \frac{1}{6} \cdot \sin^2\gamma + \frac{1}{12} \cdot \tan^2\theta_o \cdot \sin^2\gamma \right\} r dr$$

Case 6: Lateral control moment for no coning; $\beta = 0$, $\theta = \theta_o + a_1 \sin\psi$, where a_1 is small

$$M_x = \frac{3}{2} \cdot p_o\, n_b\, c \int_o^R \sin\theta_o \cdot \cos^2\theta_o \left\{ \sin 2\gamma - a_1 \left(\cos^2\gamma - \frac{1}{2} \cdot \sin^2\gamma + \frac{1}{4} \cdot \tan^2\theta_o \cdot \sin^2\gamma \right) \right\} r\,dr$$

Case 7: Spin control moment for no coning; $\beta = 0$, $\theta = \theta_o$

$$M_z = - p_o\, n_b\, c \int_o^R \sin\theta_o \cdot \cos^2\theta_o \left(\cos^2\gamma + \frac{1}{2} \cdot \tan^2\theta_o \cdot \sin^2\gamma \right) r\,dr$$

Case 8: Control forces for no coning and normal incidence of illumination; $\beta = 0$, $\gamma = 0$, and $\theta = \theta_o + b_1 \cos\psi$ where b_1 is small and constant along the span

$$F_y = - \frac{1}{2} \cdot p_o\, b_1\, n_b\, c \int_o^R \left(\cos^3\theta_o - \sin^2\theta_o \cdot \cos\theta_o \right) dr$$

$$F_z = p_o\, n_b\, c \int_o^R \cos^3\theta_o\, dr$$

Case 9: Lateral control force for no coning and normal incidence of illumination; $\beta = 0$, $\gamma = 0$ and $\theta = b_1 \cos\psi$ where b_1 is not small but is constant along the span

$$F_y = -\frac{1}{2} \cdot p_o \, n_b \, Rc \left[b_1 - 0.875 b_1^3 + 0.318 b_1^5 + - - \right]$$

The control characteristics of the Heliogyro may be illustrated by the example of the two-blade vehicle described earlier. The rate at which rotational speed can be changed by collective pitch for the condition of no coning and normal incidence of solar illumination may be computed from Case 7 above. For a 30-degree pitch angle at the blade root, the time to spin up to the final rate of 0.0175 radian per second is 3.3 days.

The rate at which the spin axis can be precessed by the simultaneous application of collective and cyclic pitch may be computed from Case 5. If the collective pitch angle is selected to be 30 degrees, and the cyclic pitch angle taken to be 10 degrees, then the precessional rate is 4.5 degrees per day.

It is shown in Case 2 that coning produces a steady moment tending to precess the spin axis in a cone about the axis of illumination. The magnitude of this moment is calculated to be 0.063 ft lb for an illumination angle of 35 degrees, and the resulting precessional rate is 0.0143 degree per day. An occasional correctional maneuver would be required on a long voyage.

Deployment

The deployment sequence for the two-blade configuration is shown in Figures 5 and 11. A small angular velocity is produced by rocket motors in order to develop initial tension in the blades. The vehicle is also oriented in space to be perpendicular to the solar radiation. Excessive spin rates would be required if the total required angular momentum were provided by the initial spin. Instead, the blades are pitched collectively after they have been unrolled a short distance. The collective pitch provides a spin torque from the photon pressure and supplies the added angular momentum needed as the blades are unrolled.

During initial deployment the angular momentum of the payload package is transferred to the unrolling blades; the spin torque is transferred primarily by chordwise bending. To preclude wrinkling of the blade, a design criterion is that there be no compressive stresses in the trailing edges during the initial deployment. For this case, the unrolling speed, $\dot{R}$, is

$$\dot{R} < \frac{\Omega_o c}{12}$$

where Ω_o is the initial rotational speed. For the case of the two-blade vehicle, this initial deployment to a radius of 326 feet must be greater than 71 seconds.

The initial deployment radius is established by the requirement that the coning angle be kept constant during the gradual payout phase, in order to minimize the deleterious effects of large coning mentioned on page 11. This criterion results in a constant ratio of blade radius to blade root stress, and in constant centripetal acceleration at the blade tip. For the two-blade configuration, if it is assumed that the initial angular momentum from rocket spinup is 900 ft-lb-sec, the resulting initial radius is 326 feet in order to assure constant tip centripetal acceleration during the remaining slow payout. The time for the complete deployment is computed to be 14.5 days based on the blade-root stress level of 1000 psi. The corresponding rotational period of the deployed Heliogyro is 6 minutes.

Spacecraft Configurations

Preliminary designs have been made of configurations of large spacecraft in order to illustrate the performance and load-carrying capabilities of the Heliogyro solar-sailer concept. The principal constraints in selecting vehicle size have been the dimensional and payload weight capabilities of the Saturn V booster system. The gross weight of the spacecraft has been chosen to be 100 000 lb and the dimensions of the stowed configuration have been selected to fit within a cylinder that is 60 feet long and 20 feet in diameter.

It has been assumed that 0.05 mil Mylar will be available for the construction of the blades. For such material, a good compromise between performance and load-carrying capability is obtained with a lightness number equal to 0.3 and a payload weight fraction equal to 0.484. Once gross weight and lightness number have been specified, the required sail area is determined. For this case, the sail area is 97.5×10^6 square feet.

The general arrangement of the first of two proposed configurations is shown in Figures 12, 13, and 14. The system consists of an

axisymmetric array of blades connected to a structural ring, and a centrally located payload capsule that is attached to the ring by means of cables. The ring is divided into 24 segments, separated by hinges. The hinges are mechanically actuated and kept in synchronism during deployment by a control cable within the ring. The cables supporting the central capsule are payed out under tension during deployment. An electrical motor that supplies blade pitch is located at the center of each ring segment. A detailed sketch of the stowed configuration is shown in Figure 14.

Operational characteristics of the pinwheel model (rotational period, tip speed,and coning angle) are included in Table II for a blade-root stress equal to 3000 psi. Final deployment from the unfolded ring condition is achieved in a manner similar to that for the experimental two-blade model. The configuration is first spun up by rocket motors to produce a moderate radial acceleration; the blades are then unrolled to a predetermined radius, pitched, and gradually payed out as photon pressure increases angular momentum. The estimated time for deployment is about eight days.

The general arrangement of the second configuration is shown in Figure 15. The system consists of a number of parallel blades with two payload capsules located half-way from the center to the blade tips. The pitch mechanisms of the blades are slaved together by a control cable that is driven by an electric motor. The blades between the two capsules are not movable. All of the blades are attached to booms that extend from the payload capsules and that are hinged to permit folding into the stowed configuration.

The axes of the movable blades are directed toward the center of rotation. The axes of the fixed blades are curved slightly outward from the center of rotation due to the action of centrifugal force.

A detailed view of the stowed configuration is shown in Figure 16. The main effect of restricted packaging volume is to limit the length of the blade attachment booms, which have been selected to have an overall length equal to 500 feet. Each boom segment carries four 10-foot-wide blades per side which could, if desired, be replaced by a single blade 40 feet wide. The total tip-to-tip span of the blades is 244 000 feet, or about 46 miles.

One important design feature of the parallel blade configuration is that artificial gravity is provided within the payload

capsules. Design data given in Table II show that, if the blade-root stress is equal to 5000 psi, the artificial gravity is equal to 0.066 g. The most effective means for providing a larger centrifugal force field is to increase blade stress, which would require the development of a suitable material that is stronger than Mylar.

TABLE II. TECHNICAL DATA FOR LARGE HELIOGYRO SOLAR SAILERS

Characteristic	Unmanned Pinwheel Model	Manned Parallel Blade Model
Gross Weight (lb)	100 000	100 000
Non-sail Weight (lb)	48 400	48 400
Lightness Number	0.3	0.3
Blade Material	1/20-mil Mylar with 1500 Å aluminum coating, each side	
Blade Area (ft^2)	97.5×10^6	97.5×10^6
Number of Movable Blades	96	80
Number of Fixed Blades	0	40
Blade Tip Radius (ft)	101 400	122 000
Blade Chord (ft)	10	10
Rotational Period (min)	18.4	17.5
Artificial Gravity for Passengers (g's)	0	0.066
Blade Root Stress (psi)	3000	5000
Blade Tip Speed (ft/sec)	568	732
Root Coning Angle (radians)	0.0048	0.00237

It will be noted that the centrifugal load on the payload capsules is supported by cables rather than being beamed to the blades. The main reason for this arrangement is that the increased load in the blades would require a reduction by about a factor of two in the artificial gravitational field. The estimated weight of the

cables, if made from unidirectional glass laminate and stressed to 100 000 psi, is about 2000 pounds.

An artist's view of one of the payload capsules is shown in Figure 17. Also visible in the figure are a cable-car for transportation to the other payload capsule, and a smaller docked spacecraft. Other features of the parallel-blade configuration that are considered to be important for long, manned space voyages are the accessibility of all moving parts and the roominess of the crew compartments.

The deployment sequence is as follows: After the blade support booms have been unfolded, the configuration is spun up by means of rocket motors at the boom tips. The non-movable blades are then payed out to a predetermined distance, after which the movable blades are payed out a small distance and pitched. Finally both sets of blades are gradually payed out as photon pressure increases angular momentum. Lag hinges for the movable blades must be provided in order to permit their axes to point toward the center of rotation during deployment.

MISSION SPECTRUM

Classification

Heliogyro applications can be classified generally by the nature of the primary function of the deployed surface. The first is related to producing thrust and orientation torques; the second is related to using the deployed solar-sail surface to intercept matter and energy. A summary of these categories of missions is given below. Specific applications are discussed in more detail in the subsequent section.

Utilization of Thrust.-

(1) Interplanetary travel

Modes: Flyby or capture

Destinations outbound: Mars, Jupiter, Saturn, asteroids, extraterrestrial moons, escape from solar system

Destinations inbound: Venus, Mercury, Sun

Destinations non-ecliptic: Comets, polar regions of solar system

(2) Travel in planetary orbit

Planetary escape

Station visiting

Orbit changing

Moon-centered satellites

(3) Station keeping and midcourse control

Interplanetary trajectory trim

24-hour orbits

Spacing of multiple satellite systems

Synodic satellites (libration points)

(4) Attitude control

Space fixed

Sun, earth or moon centered

Scanning

Utilization of surface area.-

(1) Interception of matter

Micrometeorites

Planetary atmosphere

Atmospheric density probe

Capture drag brake

(2) Interception of electromagnetic energy

Optical and radar target

Dipole and array antennas for low-frequency communication and radio astronomy

Illumination of planetary nightsides

Lunar sun shade

Effect upon local meteorology

Discussion

Utilization of Thrust for Interplanetary Travel.- Interplanetary travel requires a controlled thrust capability for midcourse orientation and trajectory control. Moreover, long-duration thrust can significantly reduce the travel time (or, for a given booster, increase the spacecraft mass) once the spacecraft is injected into

an earth-escape orbit by the primary booster. In addition, the thrust may be used to enter into and escape from high planetary orbits. Analysis shows, however, that such maneuvers are generally quite costly in time, particularly for missions to heavy planets. For instance, the descent into the earth's gravitational field requires about 700 days if the lightness number is equal to 0.1, and about 230 days if the lightness number is equal to 0.3.

Several modes of interplanetary travel can be considered, i.e, planetary flyby, planetary capture, flyby return, and capture return; the latter two modes may be considered primarily for manned explorations of the planetary system.

Destinations will affect the systems requirements for the Heliogyro. Since photon flux decreases with the square of the distance from the sun, the ability of all solar-powered propulsion systems to produce thrust diminishes rapidly on outbound journeys. Optimal sail angles are generally small (zero to 35 degrees from perpendicular to the photon flux). Deviations from specular reflectivity will therefore not seriously affect the mission performance parameters.

Typical outbound missions of primary interest are Mars, Jupiter, Saturn, asteroids, and planetary moons, particularly those of Jupiter and Saturn.

The use of the Heliogyro for solar sailing to Jupiter and beyond has been investigated in some detail by calculating a number of trajectories starting with escape from earth.

A solar sail with a $\lambda_s = 0.3$ nearly doubles the launch vehicle capability. Even $\lambda_s = 0.2$, which is almost achievable with current technology, yields a significant increase in mass. These comparisons are especially attractive when it is realized that the unpowered spacecraft must supply attitude control and midcourse correction out of its weight, whereas, the Heliogyro has these functions supplied without cost in weight. The attainable spacecraft masses are certainly impressive, even for the shorter times.

Inbound missions to Venus, Mercury, or to a still closer vicinity of the sun benefit from increased photon flux but will be limited by the sail's ability to withstand radiation equilibrium temperatures. Further investigations will be required to establish meaningful limits to such mission objectives.

A number of other trajectory profiles can be considered. These may involve ecliptic orbits with multiple flyby missions such as Venus - Mars. A multiple mission to the outer planets, Jupiter, Saturn, Neptune, and Uranus can be contemplated for the 1976 to 1978 opportunity. This opportunity will recur only in the year 2052 and therefore represents a truly exciting "once in a lifetime" opportunity for our generation. Vigorous development of the Heliogyro technology may make this concept a serious contender for inclusion into this mission.

Non-ecliptic trajectories near the sun will be of interest in surveying the otherwise inaccessible polar regions of the sun.

Interception of comets is another mission which will require deviation from ecliptic plane orbits. Two known comets that enter the inner solar system are Encke's Comet and Halley's Comet. Encke's Comet has a perihelion of 0.34 astronomical unit, an orbital inclination to the ecliptic of 12.4 degrees, and a period of recurrence of 3.29 years. Halley's Comet has a perihelion of 0.59 astronomical unit and an orbital inclination of 162.2 degrees. It is expected to recur every 76 years. Since the last well-defined observation was in 1910, the year 1986 may provide an opportunity for interception of the largest known retrograde body accessible within the confines of the inner solar system, but which is possibly of extra-solar origin.

Utilization of Thrust for Travel Within the Earth's Gravitational Field. - Use of the Heliogyro for travel in earth's orbit is less attractive than its use for interplanetary space travel due to the relatively long time required to effect large changes in orbital altitude. There are, nevertheless, a variety of transport missions within the earth's gravitational field where this disadvantage is either inoperative or relatively unimportant, and for which the large total impulsive capability and endurance of the Heliogyro present a significant advantage over other propulsion systems.

One such application is the use of the Heliogyro as a maintenance vehicle for a number of satellites stationed in synchronous orbit. The time required for a Heliogyro of relatively low performance (lightness number = 0.1) to change its orbital position by 180 degrees is equal to about 14 days. The times for smaller position changes decrease as the square root of the angle change. A competing chemical-propulsion system with a comparable payload-to-weight ratio would be exhausted of fuel after about 25 starts and stops.

Another application is the use of the Heliogyro as a logistics transport from low to high orbital altitudes in situations where the round-trip travel time is relatively unimportant. Such an application might be the ferrying of structural materials for the establishment of a base on the moon. The payload capability of the launch vehicles could be approximately doubled by using chemical propulsion to place the payload in a low (1000 mile) orbit and the Heliogyro for transfer to an orbit around the moon. The cost saving would be substantial, provided that several round-trips were accomplished by each Heliogyro transport.

Other earth-centered applications in which the special features of the Heliogyro might be advantageous are the collection of man-made debris and mapping missions that require continual changes in orbit altitude and inclination.

Utilization of Thrust for Station Keeping. - Station keeping at specific locations is a major task for long-life satellite systems, requiring small, controllable thrust over long durations. Obvious station-keeping tasks exist in present 24-hour communication satellites such as Syncom. Other unique locations for satellites are the libration points or synodic satellites in the earth-moon system.

The inferior and superior conjunction positions can be shown to be unstable, requiring an active thrust-control system. They are of particular interest as relay stations in earth-moon operations, the inferior position for communication to the near side, and the superior position for operations on the far side of the moon. The two sextile positions are inherently stable, requiring only trim and possibly damping of orbital oscillations; therefore, the control system requirement can be reduced and the Heliogyro blades may be reefed to minimize disturbances. These positions may be of interest for communication relay between earth and far side.

Locations near the opposition point may be of primary scientific interest in investigating electromagnetic and gravitational effects associated with earth-moon eclipse phenomena. These effects may be examined by observing two-body effects upon grazing rays.

Utilization of Large Surface Area for Interception of Matter. - The measurement of flux rates for meteoroids that are large enough to penetrate man-rated spacecraft requires either a very large

surface or a very long time. The blades of a Heliogyro can be used for this purpose, since their surface area must, in any case, be very large in order to provide significant thrust. The general idea is to expose the blades to the micrometeoroid flux for a certain time, and then to scan them with photoelectric devices for holes of various sizes while reeling them in. The blades would then be redeployed to collect more meteoroid holes for an additional time, etc.

A preliminary design of a vehicle for mapping the distribution of micrometeoroids between Earth and Mars has been studied. The gross weight of the vehicle would be about 730 pounds, including 280 pounds of 0.1-mil aluminized Mylar blades for primary propulsion, attitude control, and meteoroid collection; 150 pounds of thin steel plate for obtaining data for establishing correlations between hole size and penetrating power; and 300 pounds of instruments, equipment, and structure. The travel time from Earth to Mars is about 200 days. The Heliogyro blades, which have a total surface area equal to 524 000 square feet, would be scanned at two-week intervals. Calculations based on near-earth meteroid flux densities show that approximately 50 particles capable of puncturing 1 mm steel plates would be intercepted by the blades in each two-week period.

Other applications involving interception of matter involve those where the surface area is exposed to extremely tenuous atmospheres in the vicinity of planets. Such missions may have scientific value in measuring ultra-high-altitude atmospheric densities by observing orbit decay of fully or partially deployed Heliogyro-equipped spacecraft. Another application may involve the actual utilization of atmospheric drag to descend from near-parabolic to circular planetary orbits in multiple grazing orbits of initially high eccentricities, preparatory to descent to the planetary surface. Since this effect can materially reduce the weight of retropropulsion and entry heat shield, considerable payoff in mission effectiveness can be expected.

Analysis of an earth return mission shows that velocity decrements of about 1000 ft/sec per orbit can be achieved at perigee altitudes of 200 km. The time required for descent from a high orbit to a low one is thereby very substantially reduced from the time required if photon pressure is the only available propulsive effect.

Utilization of Large Surface Areas for Interception of Electromagnetic Energy. - The large surface areas available will lend themselves to applications where substantial amounts of electromagnetic radiation will be intercepted and either absorbed and reradiated or reflected either diffusely or specularly. Scientific missions using this property can involve its use as far ranging passive targets either for optical or radar tracking. Such use may serve for precise measurement of disturbing forces. From these, it is possible to determine interplanetary or planetary gravitational fields and to measure the density of extremely tenuous atmospheres surrounding planets or comets.

Another possibility exists in using the long, slender blade configurations inherent in the Heliogyro concept as dipole and array antennas for extremely low-frequency radio-astronomy studies or for deep space communication.

Interception of solar radiation may also serve direct purposes. One is that of illumination of planetary or lunar night sides. Conversely, local climate may be affected by using the large surface area to cast shadows on planetary, lunar, or earth surfaces. In the case of lunar applications, a Heliogyro placed into an approximately 28-day lunar orbit can reduce day temperature on a lunar base. Use of penumbra and appropriate blade spacing can generate a wide range of effects, from slight reduction of solar radiation to complete shadow and essentially local night situations. Modulation of the effect is possible by use of blade pitch control, inherent in the Heliogyro design. Similarly, local terrestrial meteorology may be affected by controlled removal of solar energy influx at controlled times and location. This could conceivably create or reinforce local wind patterns and be instrumental in air-pollution control. Considerable further study will be required to determine suitable orbits and magnitude of climatic effects that can be generated by this means.

Two possible modes of operation can be considered. The first involves a near-synchronous orbit of high eccentricity in which the spacecraft casts a shadow on a fixed position relative to the planetary surface. For the earth, this requires a 24-hour elliptical orbit with a major semi-axis of 6.61 earth radii, or approximately 36 000 km. For the moon, the orbital period for this mode will be approximately 28 days and the orbital semi-axis would be approximately 15 000 km.

The second mode involves lower orbits, and thus non-stationary shadows with respect to the planetary surface. To obtain sufficient effect, multiple satellite systems may have to be employed.

In either case, very large surface areas are necessary to obtain significant effects. Advances in materials technology will be required in forming thin metallic films, possibly directly in the space environment by vacuum-deposition methods.

SPECIFIC HELIOGYRO APPLICATIONS

Planetary Escape

An important and difficult maneuver that has received considerable attention in the literature on solar sails is the planetary escape maneuver (Refs. 2, 5, and 6). The reasons for the difficulty are that the gravitational attraction in a low planetary orbit is much larger than the solar-radiation pressure, and that special means are required to derive an increment of angular momentum from the sun during each revolution around the planet.

Two proposed planetary escape maneuvers for the Heliogyro are shown in Figure 18. In Figure 18(a) the vehicle is placed into a circular polar orbit with both the plane of the orbit and the plane of the vehicle normal to the direction of illumination. Cyclic pitch is used to generate a force in the direction of orbital motion. In Figure 18(b) the vehicle is placed in an equatorial orbit with the plane of the rotor normal to the direction of illumination. Both cyclic and collective pitch are employed during each orbital revolution to produce a net average force in the direction of orbital motion.

Comparison shows that the forces available for planetary escape in the polar and equatorial orbits are about equal. Slightly larger thrusts are possible with more complicated maneuvers. For example, the regions of collective and cyclic pitch could be overlapped in the equatorial orbit, or the axis of rotation could be precessed to provide a favorable orientation of the entire vehicle.

An approximate analysis of circular planetary orbits shows that the time to escape the planet from an initial orbital altitude, h_i , above the surface is

$$t_e = \frac{m_v g_o^{\frac{1}{2}} r_o}{F_\psi \left(h_i + r_o \right)^{\frac{1}{2}}}$$

where F_ψ is the average force in the direction of orbital motion, m_v is the mass of the vehicle, and g_o is the gravitational acceleration at the surface of the planet whose radius is r_o. For operation in the earth's gravitational field, the escape time is plotted in Figure 19. The importance of lightness number with regard to the time for planetary escape is clear. For manned interplanetary voyages, it is probably desirable to have the vehicle climb in an unmanned condition from a low earth orbit to a fairly high one in order to minimize radiation hazard in the Van Allen belt.

The escape time for planets other than earth may also be calculated. The escape times for the first six planets, relative to the escape time from earth, are tabulated below.

Planet	$\frac{\text{Time to Escape from Planet}}{\text{Time to Escape from Earth}}$
Mercury	0.056
Venus	0.479
Earth	1.000
Mars	1.06
Jupiter	128.0
Saturn	295.0

In a typical voyage to Mars, the spacecraft descends into a low Martian orbit, climbs back out, and returns to earth as fast as possible. The mission involves the following phases

a) Injection into a low earth orbit
b) Climb, in an unmanned condition, to a 20 000 mile orbit
c) Voyage to Mars on a capture trajectory
d) Descent to a low Martian orbit and return
e) Voyage back to earth on a flyby trajectory.

The elapsed time for the mission has been computed as a function of lightness number and is shown in Figure 20.

Interplanetary Flights

Planetary flyby missions can be considered in two phases: launch and interplanetary flight. In this analysis the launch phase is considered only to the extent necessary to establish initial conditions for the second phase. Simple two-body heliocentric orbital mechanics and flight in the ecliptic plane are assumed.

For the geometry of flight and with the notation shown in Figure 21 (a), the equations of motion may be written in non-dimensional form

$$U_{\tau\tau} - U\psi_{\tau}^{2} = \frac{\bar{D}-1}{U^{2}}$$

$$U\psi_{\tau\tau} + 2U_{\tau}\psi_{\tau} = \frac{\bar{L}}{U^{2}}$$

where the subscript, τ, denotes derivative with respect to time, and where $\bar{D}$ and $\bar{E}$ are the non-dimensional drag and lift forces on the sail, as defined below.

An element of the sail will produce lift and drag forces if it is oriented as shown in Figure 21 (b).

The elemental forces are

$$dL = \frac{\lambda}{A}\, dA \cos^{3}\varphi \cos^{2}\theta \sin\theta$$

$$dD = \frac{\lambda}{A}\, dA \cos^{3}\varphi \cos^{3}\theta$$

For trajectories which do not deviate materially from the ecliptic plane, φ is kept at its proper value over the entire sail area.

The flight vehicle can be considered to consist of the payload and the propulsion system. The propulsion system consists of the sails and the mechanisms necessary to deploy and control them. The payload mass fraction can be written

$$\frac{m_p}{m_v} = 1 - \frac{\lambda}{\lambda_s}$$

where m_p is the payload mass, m_v is the total vehicle mass, λ is the total vehicle lightness number, and λ_s is the propulsion system or sail lightness number. The sail lightness number is similar in significance to the specific impulse parameter for rocket propulsion. A specific state of solar-radiation propulsion technology can be expressed by the value of λ_s, and performance tradeoffs made relative to payload fraction and flight time.

The initial conditions for the interplanetary trajectories are a function of the performance of the launch vehicle. In Figure 22 is shown the variation of excess velocity with payload for two booster rockets, the Atlas/Centaur and the Tital IIIC - Burner II (1900). The excess velocity is related to the characteristic velocity increment, V_c, for the boosters by the equation:

$$q^2 = V_c^2 - (36178)^2$$

where the minor influence of the type of launch trajectory is not included. The Heliogyro is then assumed to escape the earth's gravitational field with an excess velocity of q at an angle β with the circle U = one astronomical unit from the sun. Thus at time zero:

$$U = 1$$

$$U_\tau = q \sin\beta$$

$$\psi_\tau = 1 + q \cos\beta$$

A sample trajectory is shown in Figure 23. The Heliogyro spacecraft reaches Mars in 83 days and Jupiter in 415 days. The sail angle is programmed so as to achieve greatest energy per unit time. This maximum power trajectory calculation offers the

simplification that the sail angle is a function only of instantaneous flight parameters. Comparison with the exact trajectory optimization of Kelley (Ref. 8) shows agreement within 2 percent. For the sample trajectory in Figure 23 the sail angle decreases rapidly from the maximum lift angle (35.3 degrees) to about 20 degrees and then decreases slowly to about 5 degrees at a distance of 10 astronomical units from the sun.

The influence of launch angle, β, and of sail angle errors were investigated (Ref. 10) and found to be minor. For example, although the optimum value of β is not zero, the penalty is small for making this simplifying assumption. For a root-mean-square deviation of sail angle of 8 degrees, the increase in flight time is about 10 percent. By making the assumptions of zero launch-angle and zero sail-angle errors, the Jupiter flyby mission can be characterized by flight time which is a function only of launch excess velocity and vehicle lightness number.

In Figure 24 are shown the basic mission results presented as flight time versus excess velocity for several values of lightness number. The curves exhibit the influence of increased lightness number in decreasing flight time. Booster performance is incorporated in the excess velocity. As shown, short flight times are possible for either the Mars or Jupiter flyby missions.

In order to introduce the performance of specific launch vehicles, the spacecraft-mass and excess-velocity data shown in Figure 22 may be combined with the basic mission results. Consider a requirement in which a given payload mass is to be flown near Jupiter with a given booster and utilizing a basic solar-sailing capability. In order to find the minimum flight time, data as shown in Figure 25 may be computed and plotted. In this case the Titan IIIC-B2 and a payload mass of 227 kg for the Heliogyro were selected. By varying the lightness number, the minimum flight time may be found as shown.

In Figure 26 the optimum flight times for specified payloads are shown for various sail lightness numbers. Each point on these curves represents an optimum point selected from curves shown in Figure 25. The results apply to the Jupiter flyby mission utilizing either the Titan IIIC-Burner 2 or the Atlas/Centaur launch vehicle.

The curves in Figure 26 for the sail lightness number, $\lambda_s = 0$, give the ballistic performance of the Titan booster without solar-sail propulsion. Addition of solar sails will appreciably increase

the payload weight capability or reduce the flight time.

The curves in Figure 26 for the Atlas booster were selected to show a near-future capability. A value of $\lambda_s = 0.15$ can be obtained with presently available materials, and $\lambda_s = 0.3$ could be obtained with polymer films of one-tenth mil. A 400-kilogram payload could be placed in the vicinity of Jupiter with the Atlas/Centaur. The Heliogyro would weigh 945 kg, have a vehicle lightness number of 0.17, and a sail area of 0.1 square kilometer. For comparison, the performance characteristics of a solar-powered electric propulsion system for the Jupiter flyby mission are also shown. Data are taken from Reference 13 and reflect direct, outbound trajectories, optimized for launch date and maximum gross payload.

Attitude Control

The application of the Heliogyro to attitude control was suggested by the successful employment of solar radiation for this purpose on the Mariner program. In this study, consideration has been given to applications requiring simultaneous application of large forces and moments about two or three axes.

The example chosen for investigation was the lateral control system for a large radio-astronomy antenna, the LOFT (see Ref. 11). This orbiting low-frequency telescope has a diameter of 1500 meters and is required to scan the celestial sphere and to point at specific objects in space. The configuration chosen for analysis is shown in Figure 27. It will be noted that the Heliogyro blades spin in a direction opposite to that of the scanning antenna. This is done in order to reduce the net angular momentum of this system to zero thereby minimizing control torque requirements.

In this case the moment requirements are of two types: torque about the spin axis, and moment about an axis perpendicular to the spin axis. Torque about the spin axis is required to bring the antenna up to the desired spin rate. Spin torque will also be required during subsequent operation to replenish losses in angular momentum due to eddy current interaction with the earth's magnetic field.

Lateral control moments (pitch and yaw) are required to change the pointing axis of the antenna and also to overcome moments produced by the natural environment. The major sources of environmental lateral moment are gravity gradient and solar-radiation pressure. The magnitude of the required control moment can vary

depending on several parameters. Some of the more important parameters are:

1. Orbital altitude: gravity-gradient torque is inversely proportional to the cube of the distance from the center of the earth.

2. Mass distribution: gravity-gradient torque can be reduced to nearly zero by making the moments of inertia about the spin axis and a transverse axis nearly equal.

3. Distribution and area of antenna reflecting surfaces determine the moment due to solar-radiation pressure.

The origin and magnitude of lateral control moment under different design conditions are given below.

Design Conditions	Moment Required to Overcome:			
Orbital Altitude	Inertia	Gravity Gradient	Radiation Pressure	All Effects
	(ft-lb)			
6000 km	2	15	10	27
34 000 km (synchronous)	2	0.5	10	12

The lateral-control moment system must be capable of slewing the antenna between any two orientations in less than one day. This requirement rules out systems that depend entirely on environmental forces (such as gravity-gradient schemes), but it does not rule out systems (such as rocket-motor propulsion) that take advantage of environmental forces to reduce the long-time average moment. All systems must be capable of delivering the maximum required moment at any time. The duration of the mission is assumed to be five years.

For the Heliogyro attitude-control configuration on LOFT as shown in Figure 27, the reflector blade pitch is controlled as follows:

$$\theta = \theta_o + a_1 \sin\psi + b_1 \cos\psi$$

where $\psi = \Omega\tau$ is measured from a reference plane that contains the axis of rotation and the direction of the illumination. The control parameters, θ_o, a_1, and b_1 are called, respectively, collective pitch, longitudinal cyclic pitch, and lateral cyclic pitch in conformity with standard helicopter practice.

There are two modes of control that will produce a lateral moment on the antenna. In the first mode a lateral force is produced on the reflector blades which, when multiplied by the distance between the plane of the reflector and the center of gravity of the antenna, produces the desired moment. In the second mode the components of force on the blades in the direction of the axis of the antenna are modulated differentially so as to produce a moment when they are multiplied by the distance from the blades to the axis. The formulas for the control moments about the y-axis are:

Mode 1: $\theta = a_1 \sin\psi$

$$M_y = \frac{1}{2} a_1 p_o n_b c(R_2 - R_1) \ell_{cg} \cos^2\gamma$$

Mode 2: $\theta = \theta_o + b_1 \cos\psi$

$$M_y = \frac{3}{4} b_1 p_o n_b c (R_2^2 - R_1^2) \sin\theta_o \cos^2\theta_o (\cos^2\gamma - \frac{1}{6}\sin^2\gamma + \frac{1}{12}\tan^2\theta_o \sin^2\gamma)$$

where a_1 = longitudinal cyclic pitch

b_1 = lateral cyclic pitch

θ_o = collective pitch

p_o = radiation pressure for normal incidence

n_b = number of blades

c = blade chord

R_1 = inner blade radius

R_2 = outer blade radius

ℓ_{cg} = distance from blade plane to c.g. of antenna

γ = angle between axis of antenna and direction of the solar illumination

ψ = $\Omega\tau$

Ω = rotational speed

τ = time

The formulas for the moments about the x-axis are similar.

In the derivation of the above formulas it is assumed that the cyclic pitch angles, a_1 and b_1, are small. Although the collective pitch angle, θ_o, varies along the span, a weighted average is assumed in these formulas. For purposes of evaluating the performance of the design concept, the following numerical values were selected for the parameters listed above.

a_1 = 20°

b_1 = 20°

θ_o = 30°

p_o = 0.1882 x 10^{-6} lb/ft^2

n_b = 3

c = 10 ft

R_1, R_2: to be determined by moment requirements

ℓ_{cg}: 1500 ft

γ : all values to be considered

Consider Control Mode 1. The average value of $\cos^2\gamma$ over the surface of a sphere is 1/3. Thus the average moment capability is

$$\bar{M}_y = \frac{1}{6} a_1 p_o n_b c \ell_{cg} (R_2 - R_1)$$

$$= 5.14 \times 10^{-4} (R_2 - R_1)$$

The following table gives pertinent design information for various values of $\bar{M}_y$. Quarter mil aluminized Mylar is assumed in calculating blade weights.

$\bar{M}_y$ (ft-lb)	$R_2 - R_1$ (ft)	Surface Area of Three Blades (ft^2)	Weight of Three Blades (lb)
1.0	1 950	58 500	114
10.0	19 500	585 000	1 140
100.0	195 000	5.85×10^6	11 400

Consider Control Mode 2. The average absolute value of $(\cos^2\gamma - \frac{1}{6}\sin^2\gamma + \frac{1}{12}\tan^2\theta_o \sin^2\gamma)$ over the surface of a sphere is approximately 0.306. Thus the average moment capability is

$$\bar{M}_y = \frac{3}{4} \times 0.306\, b_1 p_o n_b c \sin\theta_o \cos^2\theta_o (R_2^2 - R_1^2)$$

$$= 1.76 \times 10^{-6} (R_2^2 - R_1^2)$$

Clearly the inner radius should be made as large as practical in order to produce the maximum moment. Using a value of 10 000 ft,

$$\bar{M}_y = 17.6 \left[\left(\frac{R_2}{R_1} \right)^2 - 1 \right]$$

The following table gives pertinent design information for various values of $\overline{M}_y$. Quarter mil aluminized Mylar is assumed in calculating blade weight.

$\overline{M}_y$ (ft-lb)	$\frac{R_2}{R_1}$	$R_2 - R_1$ (ft)	Surface Area of Three Blades (ft^2)	Weight of Three Blades (lb)
1.0	1.028	280	8 400	19.4
10.0	1.253	2 530	75 800	148.0
100.0	2.585	15 850	475 000	924.0

The second control mode leads to a much smaller blade weight than the first control mode. The weight of a complete system to produce 10 ft-lb of lateral moment should be no more than about 250 lb.

Two other candidate lateral-control systems, rocket motors and interaction with the earth's magnetic field, were evaluated for application to the LOFT. It was concluded that chemical rockets could not be used due to excessive weights. At synchronous altitudes electrical-propulsion rockets would be competitive in weight if specific impulses in the range of 5000 to 8000 seconds could be developed. The magnetic interaction system is lightest at the low orbiting altitude of 6000 kilometers. The solar-reflector system is the lightest system for the synchronous altitude and can also provide the forces and moments needed for station keeping.

Micrometeoroid Survey

The use of a Heliogyro for a detailed meteoroid flux survey in the solar system is of interest since the spacecraft has the ability to explore various regions at will, and to return to near-earth space for transmission of stored data. Because the large areas of the blades will record meteoroid size rather than mass, an additional array of steel plates is provided so that correlation between particle diameter and penetrating power can be made.

Measurement of flux rates for meteoroids which are large enough to penetrate spacecraft requires either large surface areas or long times. Since the surface area of the blades of the Heliogyro must in any case be very large in order to provide sufficient thrust, the concept of scanning the solar sail for holes of various sizes has been investigated.

The accumulation of holes in the thin Mylar blades may be measured and counted by photoelectric devices to determine micrometeroid flux rate as a function of particle diameter. Since the surface area is very large, the statistical distribution of particle size can be determined to a high degree of accuracy. By redeploying the blades at frequent intervals, information on the particle size distribution as a function of distance from the sun and planets could be obtained.

In order to obtain information on the distribution of particles by penetrating power, additional apparatus may be carried along to measure the number of penetrations of steel plates of different thicknesses. Such apparatus cannot obtain the same quantity of information as is provided with regard to particle size by the Mylar sheets, except at prohibitive weight. (See Fig. 28). However, a correlation between particle diameter and penetration power may be established so that the large amount of information collected by the Mylar blades can be used to assist in calculating penetrating power distribution. The mass addition to the spacecraft will thereby be minimized.

To establish a method of correlation, let it be supposed that average flux rates with regard to penetrating power and to particle diameter are measured by independent means for the same time span and the same flight trajectory (i.e., by independent experiments on board the same spacecraft). The flux rates N_d (number of particles per unit area with diameter larger than d) and N_t (number of particles per unit area penetrating a plate of thickness, t) can then be graphed as shown in Figure 29.

The distributions are shown as bands of varying widths, indicating the variation of statistical reliability of the measurements.

A correlation between diameter, d , and plate thickness, t , is postulated in the form

$$t = f(d) \cdot d$$

Let $f(d)$ be plotted from the available experimental data for equal values of flux, i.e., for $N_d = N_t$. The graph of t versus d will have the general appearance shown in Figure 30.

For small particles, the variance of plotted points from a smooth curve will be small due to the large number of measured points (particle flux is approximately inversely proportional to the cube of particle diameter). For large particles the variance of t is presumed to be so large that the measured data are inadequate. The smooth curve obtained for small particles is extrapolated into the large particle range, taking some account of the measured data in that range.

The resulting smoothed curve of $f(d)$ is then used with the distribution of particle diameter to produce the distribution of particle penetrating power. The curve of $f(d)$ versus d is used for situations other than the one from which it was derived, i.e., for shorter time intervals and for localized regions of space.

Inherent assumptions are that the mean particle density is relatively insensitive to particle size, and that the mean particle density does not vary greatly between different locations in space. No assumption is made, and indeed nothing can be learned about the density distribution of particles with the same mass. All that is said is that particle flux based on penetrating power and particle flux based on diameter are statistically correlated and that the experimentally observed correlation can be extrapolated with respect to particle size and with respect to location in space. The experiments themselves can determine whether these assertions are valid.

As a baseline concept, it is assumed that the system must obtain reliable statistics for the distribution of meteoroids that are capable of penetrating a one millimeter steel plate. Technical data reviewed in Reference 12 shows that for a wide range of conditions, the plate thickness for penetration is related to particle mass by the empirical formula

$$t_p = 1.56 \left(\frac{m_p V_p^{\frac{3}{2}} V_o^{\frac{1}{2}}}{4\pi F_{tu}} \right)^{\frac{1}{3}}$$

where m_p = mass of particle

V_p = velocity of particle

$V_o = 0.65 \times 10^6$ cm/sec

F_{tu} = ultimate tensile strength of target.

If it is assumed that

$$V_p = 3 \times 10^6 \text{ cm/sec}$$

as determined from meteor observations by Whipple, et. al., and

$$F_{tu} = 10^{10} \text{ dynes/cm}^2 \text{ (142 000 psi)}$$

then the particle mass that will produce penetration in a 1 mm plate is 7.9×10^{-6} gram.

Recent data obtained near the earth indicate that the flux rate for particles with mass greater than m_p (grams) is about:

$$N_p = 10^{-14}/m_p \text{ particles/m}^2\text{/sec}$$

Thus the estimated flux rate for particles that will penetrate a 1 mm steel plate is

$$N_p = 10^{-14}/7.9 \times 10^{-6} = 0.127 \times 10^{-8} \text{ particles/m}^2\text{/sec}$$

Assume that measurements of the number of holes produced by meteoroids are made at two-week intervals and that 50 holes will provide sufficiently reliable statistics. For a reasonably high probability of counting 50 holes, the required surface area is

$$A = \frac{70}{\text{flux time}} = \frac{70}{0.127 \times 10^{-8} \times 14 \times 24 \times 3600} = 45\ 700\ m^2$$

$$= 493\ 000\ ft^2$$

This corresponds to a size requirement of a Heliogyro weighing about 1000 pounds.

An experimental vehicle for micrometeoroid surveys might include:

1. 280 lbs of 0.1 mil aluminized Mylar with a surface area equal to 350 000 ft^2.

2. 150 lbs of steel plates.

3. 300 lbs of instruments, equipment, and structure.

The gross weight is 730 lbs and the lightness number is λ = 0.148. The travel time from earth to Mars on a flyby mission is about 200 days. The time required to scan the region within the earth's effective gravitational field is about 450 days.

This Heliogyro (see Fig. 31) would have 4 blades with ten-foot chord and 12 400 foot radius. Four blades are recommended rather than two in order to reduce changes in tip speed and centrifugal stress during blade reefing. One pair of blades would be deployed while the other pair is reeled in. Thus angular momentum will be maintained without large changes in angular velocity.

Atmospheric Braking

The time required for a Heliogyro to descend from a high circular planetary orbit to a low one is rather long if photon pressure is the only propulsive effect employed. It has been shown that descent into the earth's gravitational field requires about 700 days if the lightness number is equal to 0.1, and about 230 days if the lightness number is equal to 0.3. The large surface areas of the Heliogyro suggest that the descent time can be significantly reduced by atmospheric braking.

Direct entry into the atmosphere and descent to the surface from a parabolic or hyperbolic orbit is not a practicable maneuver for the Heliogyro, due to the low strength of the long, slender

blades. The peak deceleration encountered during descent from even a very low circular orbit is about eight g's, while the maximum deceleration capability of the Heliogyro is less than one g. For direct entry of the Heliogyro into a planetary atmosphere some means other than thin Mylar blades must be provided to protect the craft from high loads and temperature during entry.

A more promising maneuver is to place the vehicle into a parabolic orbit that intersects the upper planetary atmosphere such that a small decrease in velocity occurs in conjunction with a small peak deceleration. The vehicle will then describe an elliptic orbit about the planet and reenter the planetary atmosphere at the same velocity and entry angle at which it departed. Succeeding orbits will have decreasing ellipticity and period. Eventually the vehicle will be captured by the atmosphere. Alternately, after several braking orbits its control system can produce a circular orbit outside the sensible atmosphere.

The time required for the maneuver can be calculated in terms of the velocity decrement per orbit. The period of the elliptic orbit is

$$\tau = \frac{\tau_c}{\left[2 - \left(\frac{v}{v_c}\right)^2\right]^{3/2}}$$

where v is the velocity at perigee in an elliptic orbit, v_c is the velocity of a circular orbit with altitude equal to the perigee and τ_c is the period of the circular orbit.

As an example, consider an earth entry for which $\tau_c = 1.42$ hrs and $v_c = 25\,000$ ft/sec. Let the velocity decrement be 1000 ft/sec and assume that the initial trajectory is parabolic, $v_o = \sqrt{2}v_c$. Then the time for succeeding orbits is as shown below.

Orbit No.	Perigee Velocity (ft/sec)	Time (hrs)
1	34 000	35.4
2	33 000	13.5
3	32 000	7.5
4	31 000	5.0
5	30 000	3.7
6	29 000	2.9
7	28 000	2.3
8	27 000	2.0
9	26 000	1.7
10	25 000	1.5 ←——capture
	TOTAL	85.5 hrs

In the example, the time for the first orbit accounts for 41.4% of the total time. The time for the first orbit depends on the velocity decrement as follows,

$$\tau_1 = \frac{\tau_c}{4.76}\left(\frac{v_c}{\Delta v}\right)^{3/2}$$

or

$$\Delta v = v_c \cdot \left(\frac{\tau_c}{4.76\tau_1}\right)^{2/3}$$

If, for example, the time for the first orbit is 20 days (480 hrs), the required velocity decrement computed is 182 ft/sec.

Consider next the relationship between velocity decrement and peak deceleration during a grazing encounter with a planetary atmosphere. Figure 32 shows geometrical relationships near perigee of a parabolic trajectory. The trajectory is equidistant between

the circle with altitude equal to perigee and its tangent plane. Thus, for the angle $\varphi << 1$,

$$\Delta z = R_p \cdot \frac{1 - \cos\varphi}{1 + \cos\varphi}$$

$$\simeq \frac{1}{4} \cdot R_p \varphi^2$$

where R_p is the perigee radius.

If the velocity decrement is very small, the peak deceleration will occur approximately at perigee and will be proportional to atmospheric density. Thus the deceleration is

$$a = gN_{max} \cdot \frac{\rho}{\rho_{z_o}}$$

where N_{max} is the peak load factor in g's and ρ is the atmospheric density. Assuming an exponential variation of atmospheric density,

$$\frac{\rho}{\rho_{z_o}} = e^{-\frac{\Delta z}{H}}$$

where H is the scale height.

Then the velocity decrement is

$$\Delta v = \frac{2gN_{max}}{v} \cdot \sqrt{\pi R_p H}$$

As an example, consider an earth entry with $N_{max} = 0.1$ g , v = 36 000 ft/sec , and $R_p = 20 \times 10^6$ ft.

Then

$$\Delta v = 636 \text{ ft/sec},$$

which is sufficient for a satisfactory maneuver time.

The maximum permissible deceleration is related to design parameters by

$$N_{max} = n_b \cdot \frac{\sigma_o t\, c}{W_p} \cdot \sin\beta_{max}$$

where σ_o is the stress at the blade root, t , is blade thickness, c is blade chord, n_b is the number of blades, and β_{max} is the maximum value of the coning angle at the root of the blade, and W_p is payload weight.

As an example assume

$n_b = 4$
$\sigma_o = 5000$ psi
$t = 10^{-4}$ inch
$c = 120$ inches
$\beta_{max} = 1.0$ degree
$W_p = 500$ lb

Then $N_{max} = 0.083$ g.

The perigee radius, z_o , is determined by the maximum permissible deceleration

$$N_{max} = \frac{1}{2} \cdot \rho_{z_o} v^2 \cdot \frac{A}{W}$$

For this example assume

$$A = 350\ 000\ ft^2$$

$$W = 730\ lb$$

$$v = 35\ 000\ ft/sec$$

$$N_{max} = 0.083$$

Thus,

$$\rho_{z_o} = \frac{2 \times 0.083 \times 730}{(350\ 000) \times (35\ 000)^2} = 2.82 \times 10^{-13}\ lb\text{-}sec^2/ft^4$$

$$= 8.8 \times 10^{-12}\ lb/ft^3$$

which, corresponds to an altitude of about 230 km.

CONCLUDING REMARKS

In summary, design concepts for a new type of space vehicle have been introduced, and a spectrum of possible applications with wide utility have been suggested. It appears that the weight and performance advantages of the Heliogyro for long space missions warrant additional work in the development of the concept technology.

There are a number of areas in which additional work remains to be done in order to establish technical feasibility. One of the areas of concern is the effect of blade deformation on controllability. It has been shown, for example, that in the absence of bending deformations, a collective pitch angle imposed at the root of a blade is propagated to the tip of the blade by centrifugal stiffening. The extent to which flapwise and chordwise deformations interfere with the spanwise propagation of blade pitch is not known at present. A fully coupled analysis, including dynamic effects, is required in order to obtain such knowledge.

Although currently available materials appear to be adequate for the design of Heliogyro blades, significant increases in performance could be obtained with better materials. Reduction of film thickness is an obvious goal that will produce either shorter mission times or larger payload weight fractions. The development of films with higher strength is also desirable, particularly for larger vehicles.

The preliminary survey of the mission spectrum for a Heliogyro has revealed an array of possible applications. Interplanetary travel, station keeping, attitude control, interception of micrometeoroids or electromagnetic energy, and atmospheric braking have been briefly evaluated. The most interesting application involves the "space cruiser" concept suggested by Mr. Norman J. Mayer, of NASA Headquarters, in December 1967. This broader mission role encompasses multiple objectives over a long term and provides considerable latitude in choosing orbits, trajectories, and specific missions. The independence of the Heliogyro concept from fuel requirements and the multiplicity of its potential applications are well suited to this role. It appears, therefore, that the development of the Heliogyro-concept technology into practical hardware is warranted, and that further mission studies should be made in order to establish definitive technical and operational criteria.

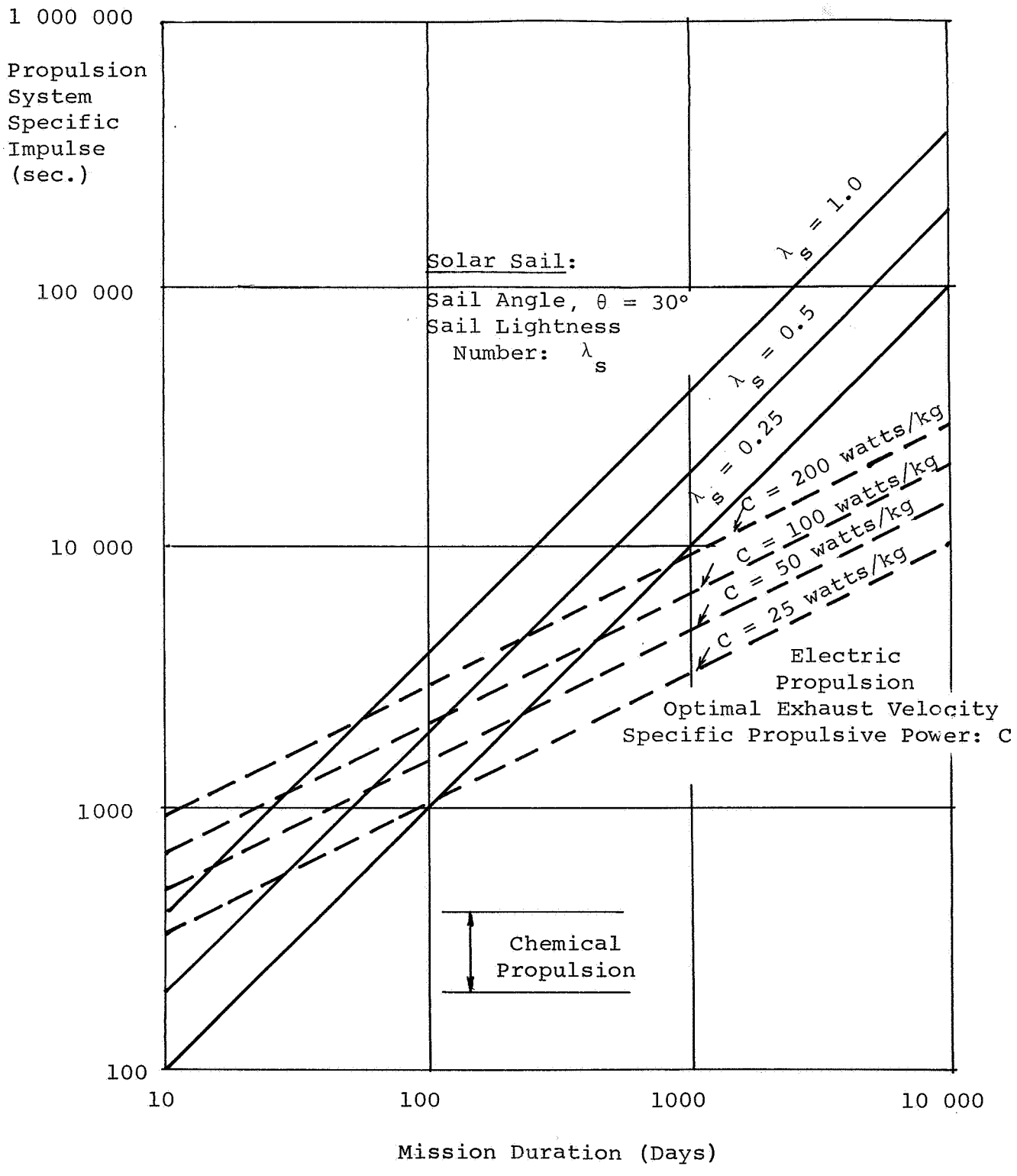

Figure 1. Specific Impulse of Propulsion Systems Operating in the Vicinity of the Earth's Orbit

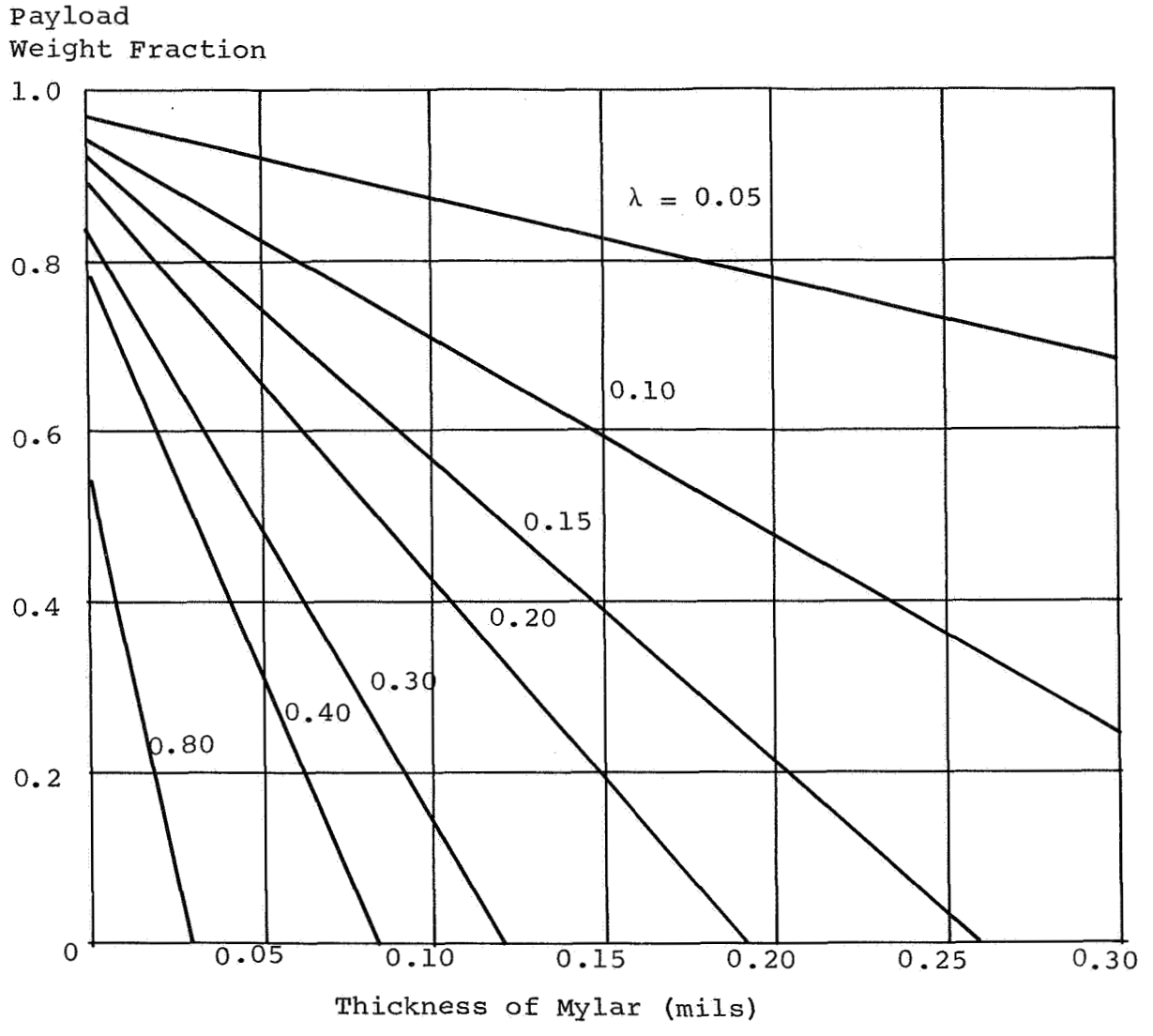

Figure 2. Payload Weight Fraction vs. Thickness of Mylar Sheet

Thickness of Aluminum = 3000 Å

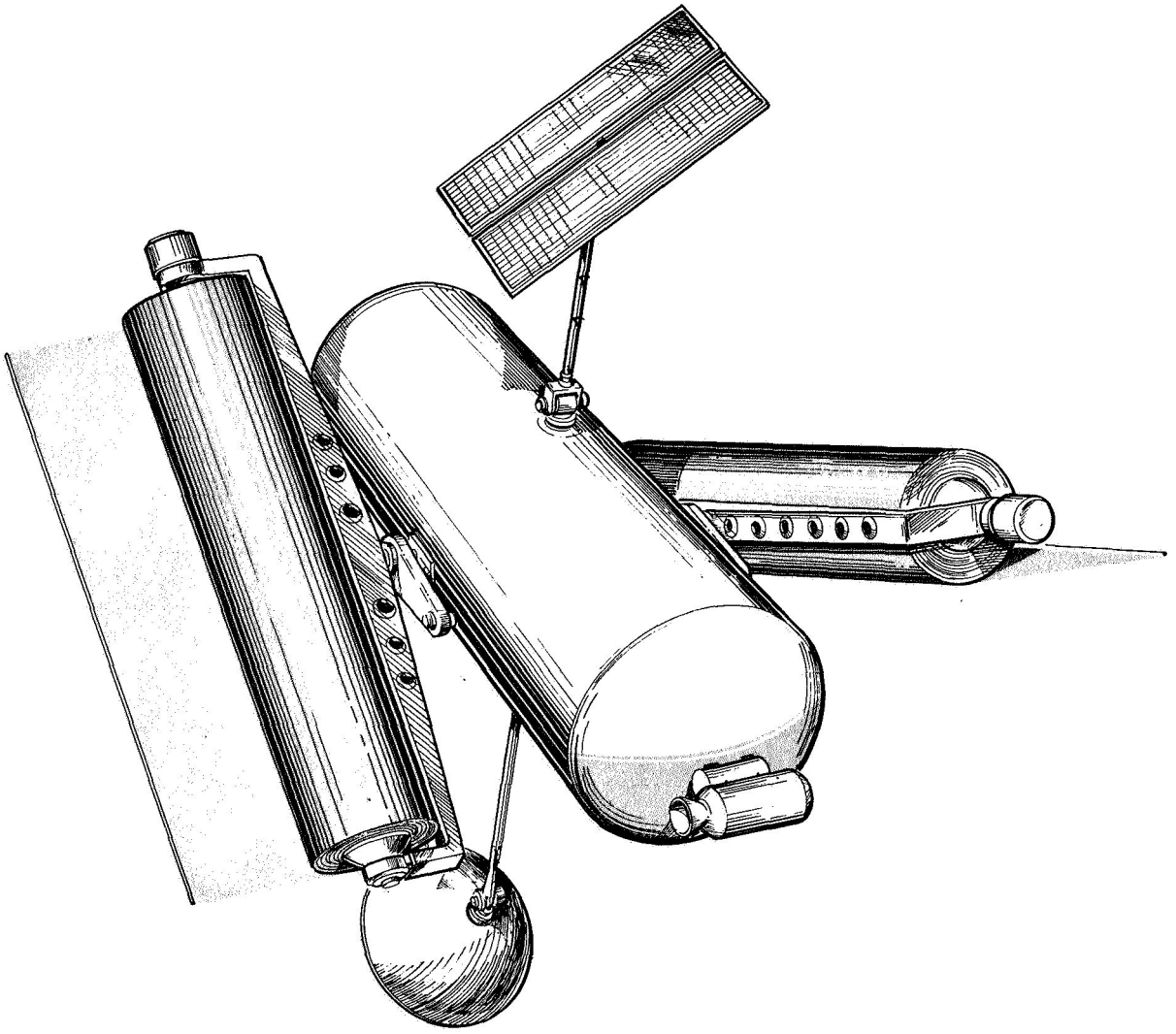

Figure 3. Sketch of Experimental Two-Blade Model

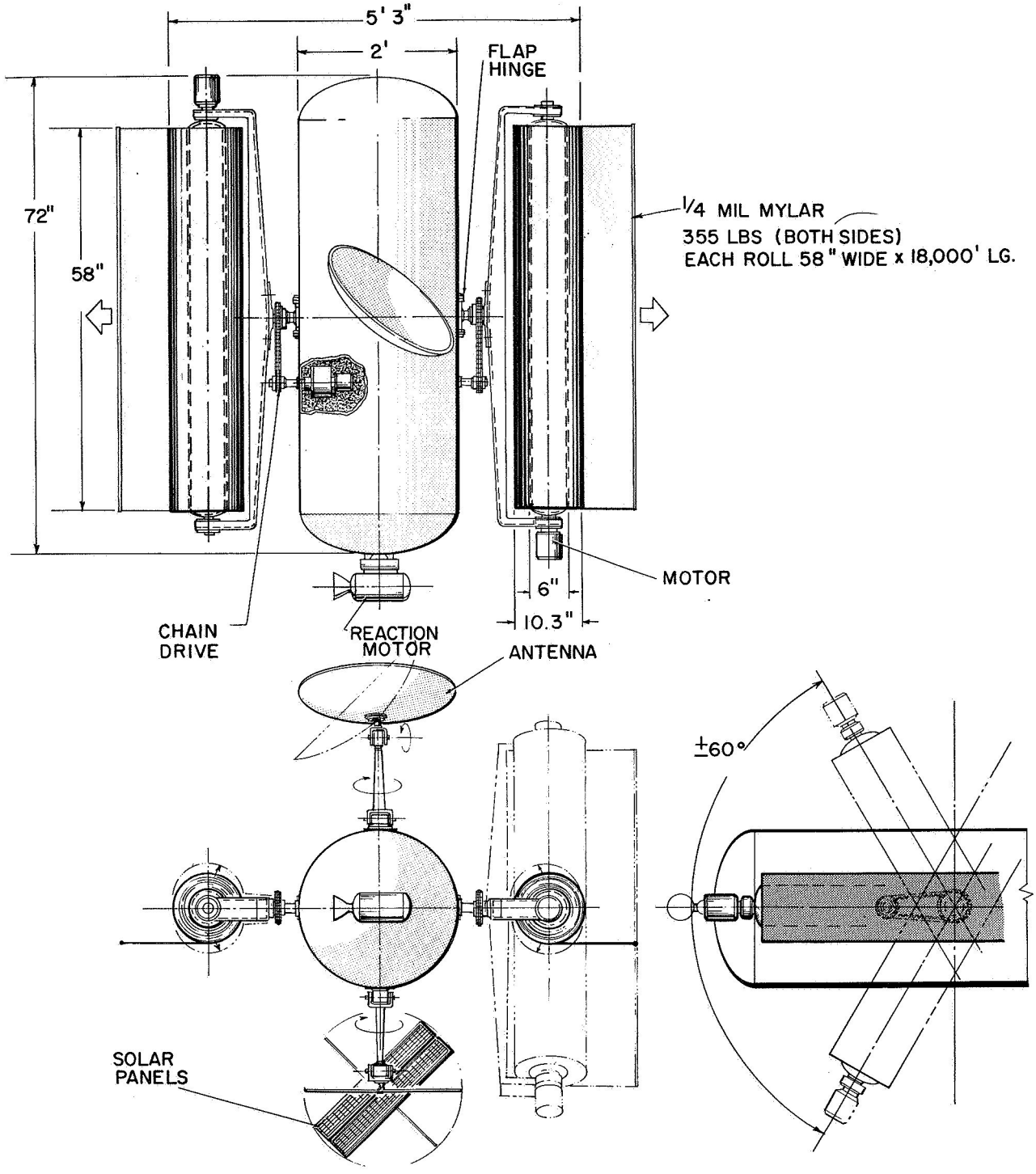

Figure 4. Three Views of Experimental Two-Blade Model

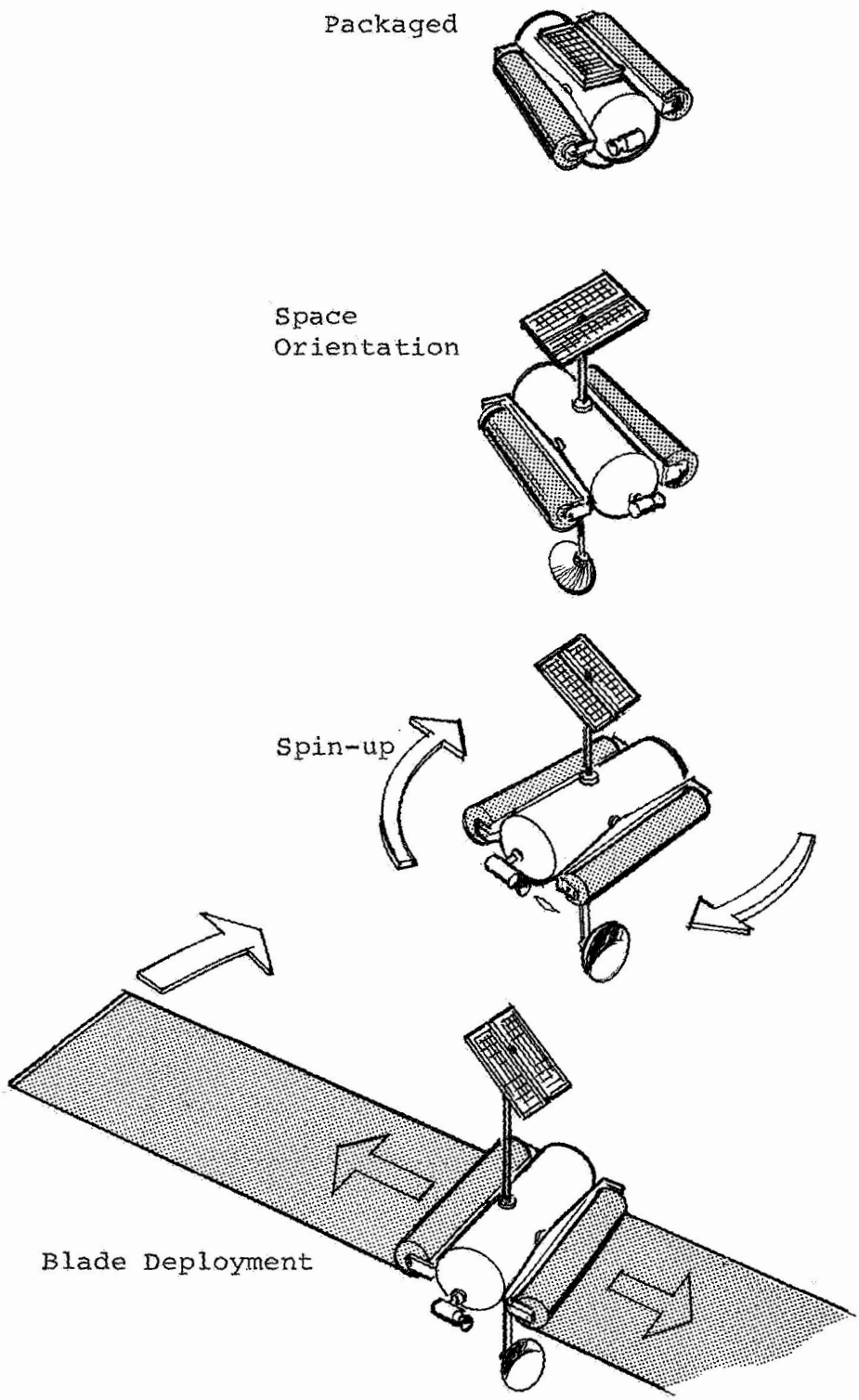

Figure 5. Deployment Sequence for Two-Blade Model Heliogyro

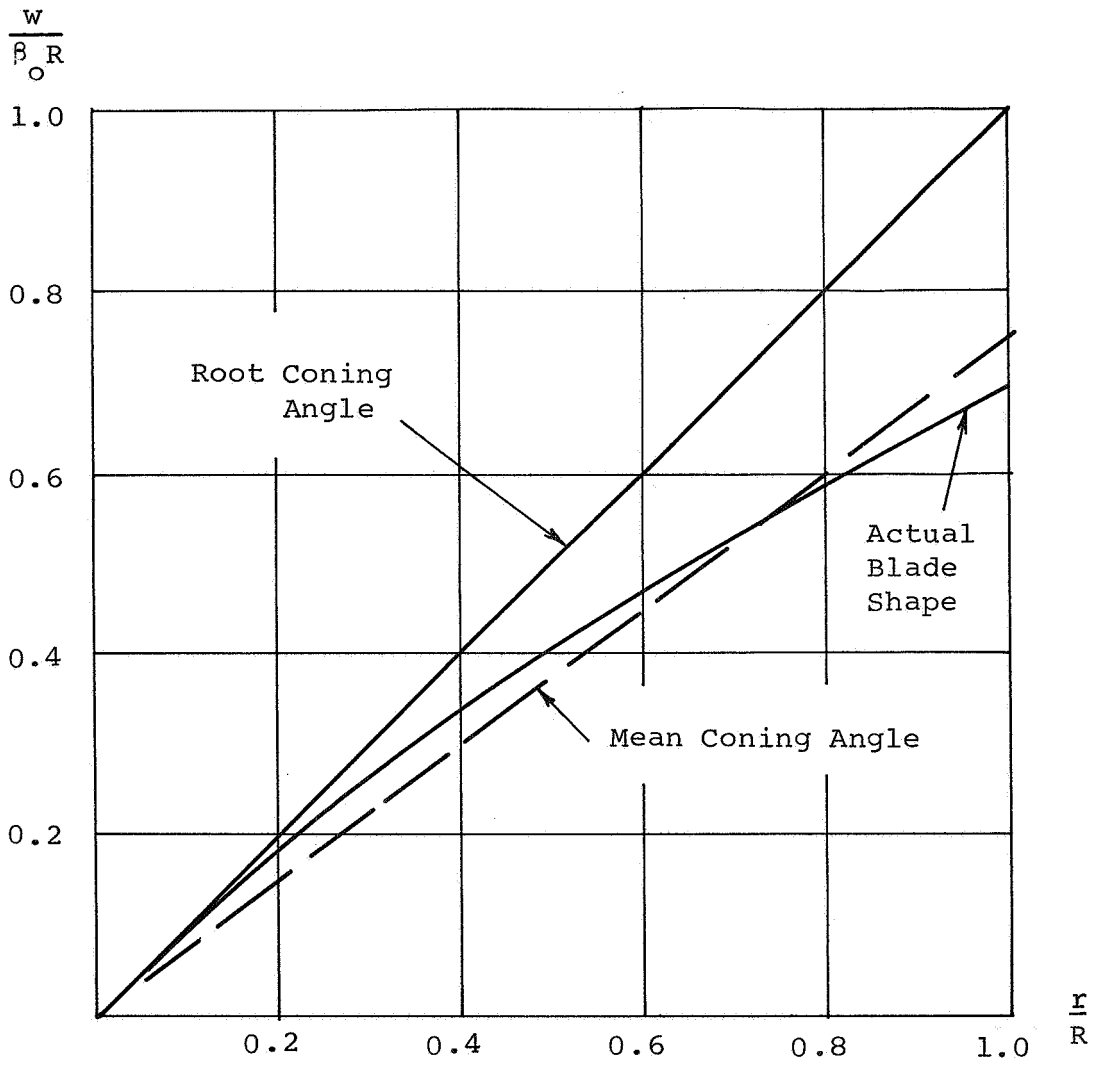

Figure 6. Vertical Blade Deflection for Two-Blade Model Vehicle

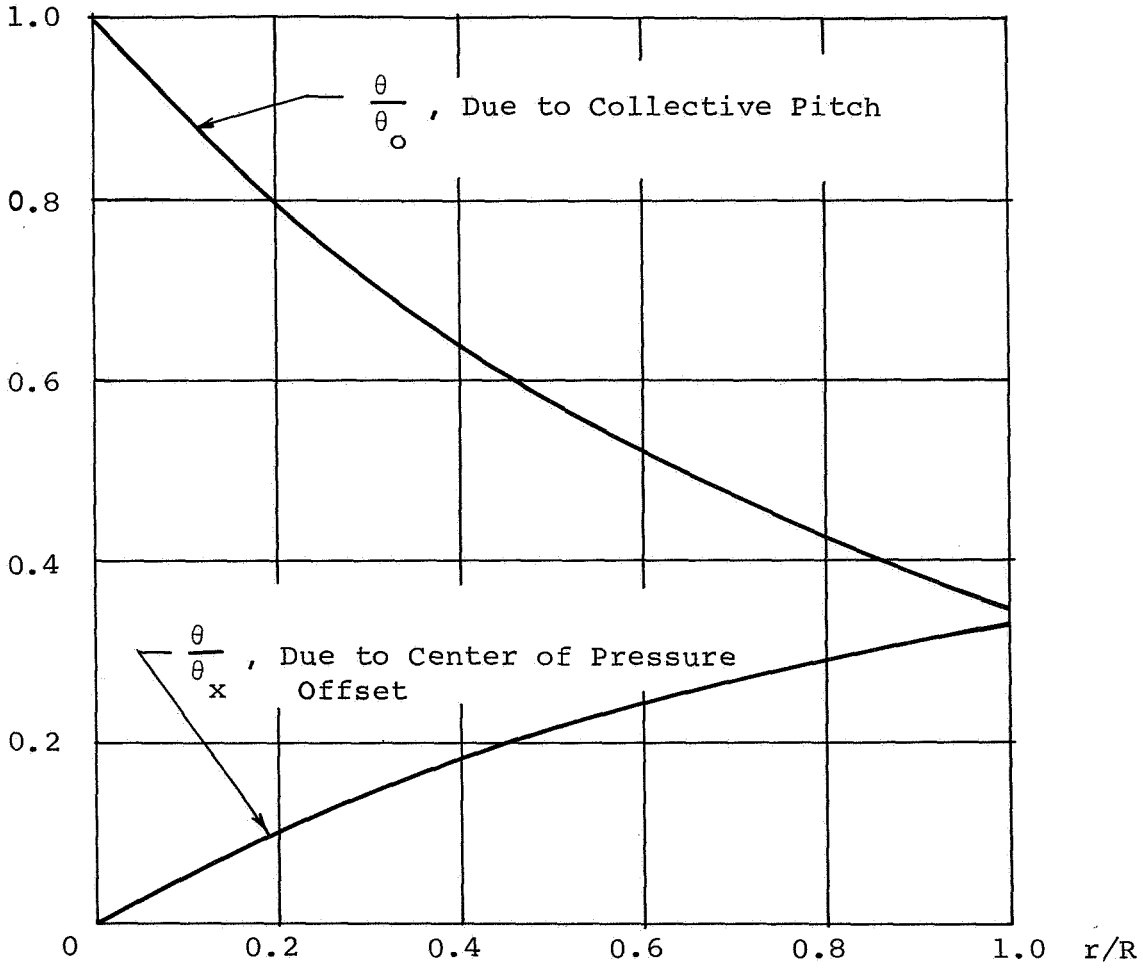

Figure 7. Blade Twist

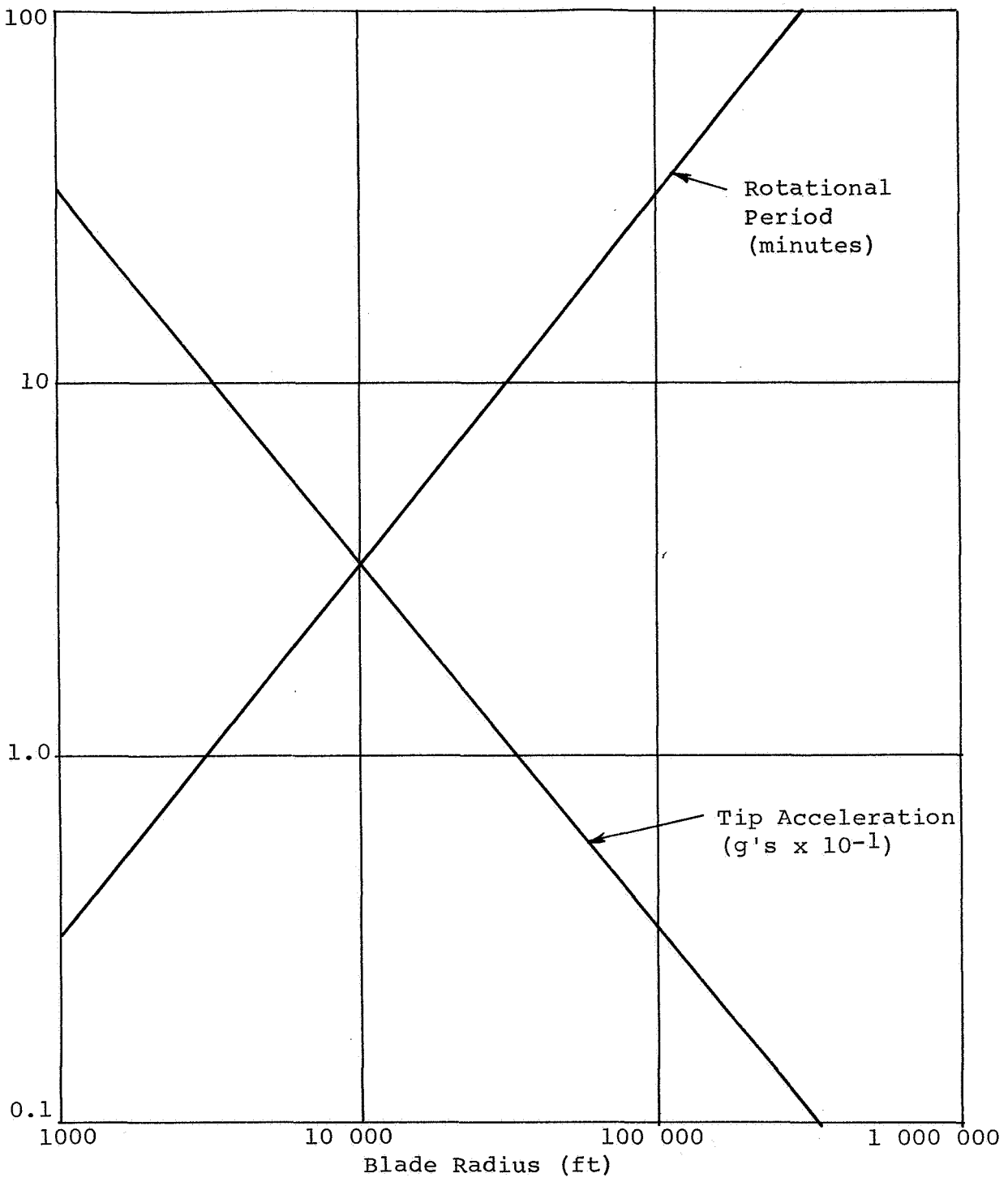

Figure 8. Operational Characteristics of 1/4-mil Mylar Blade with 1000 psi Root Stress

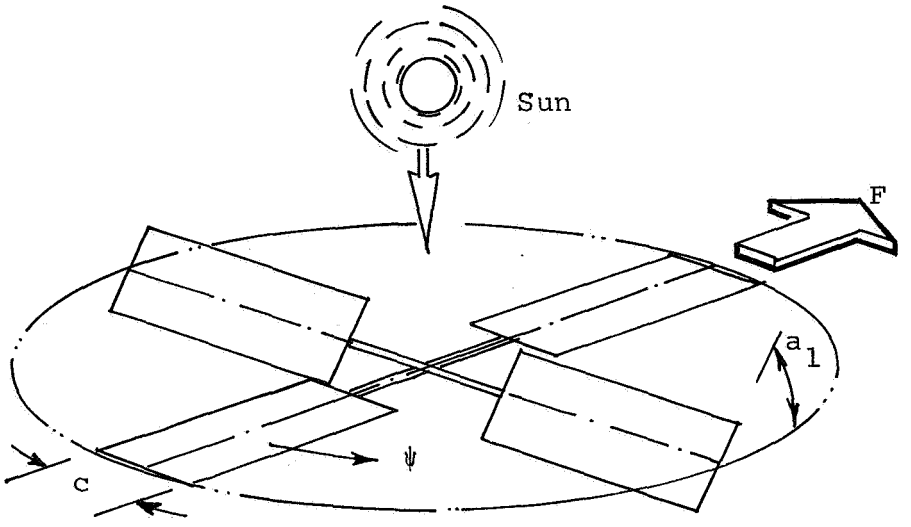

a) Lateral force produced by cyclic pitch. $\theta = a_1 \sin\psi$

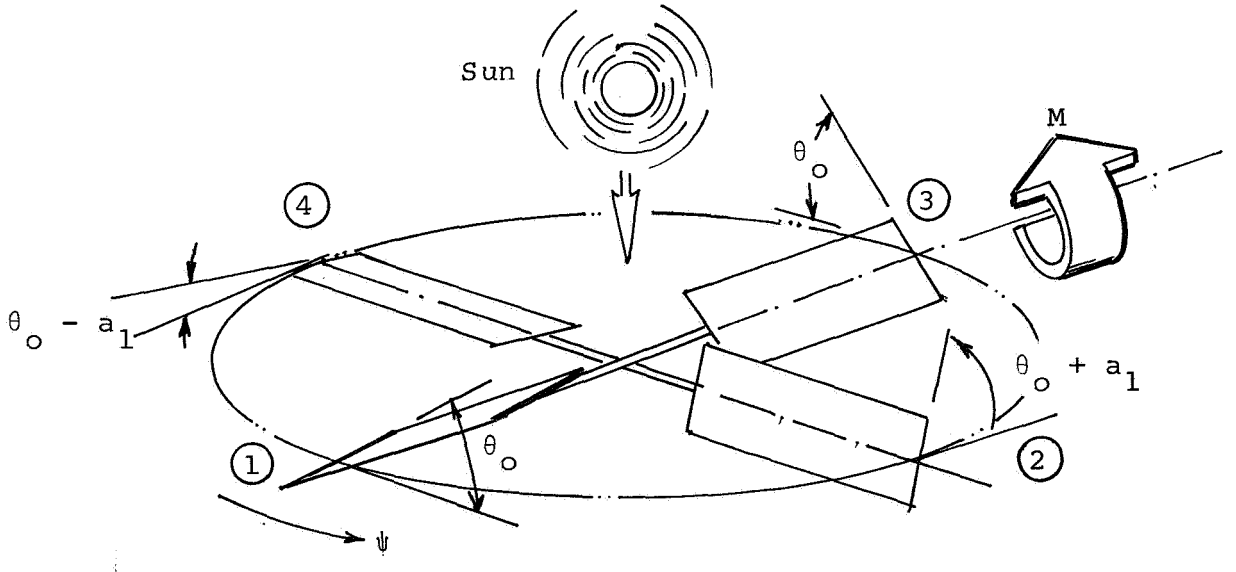

b) Rolling moment produced by combined collective and cyclic pitch. $\theta = \theta_o + a_1 \sin\psi$

Figure 9. Control Responses

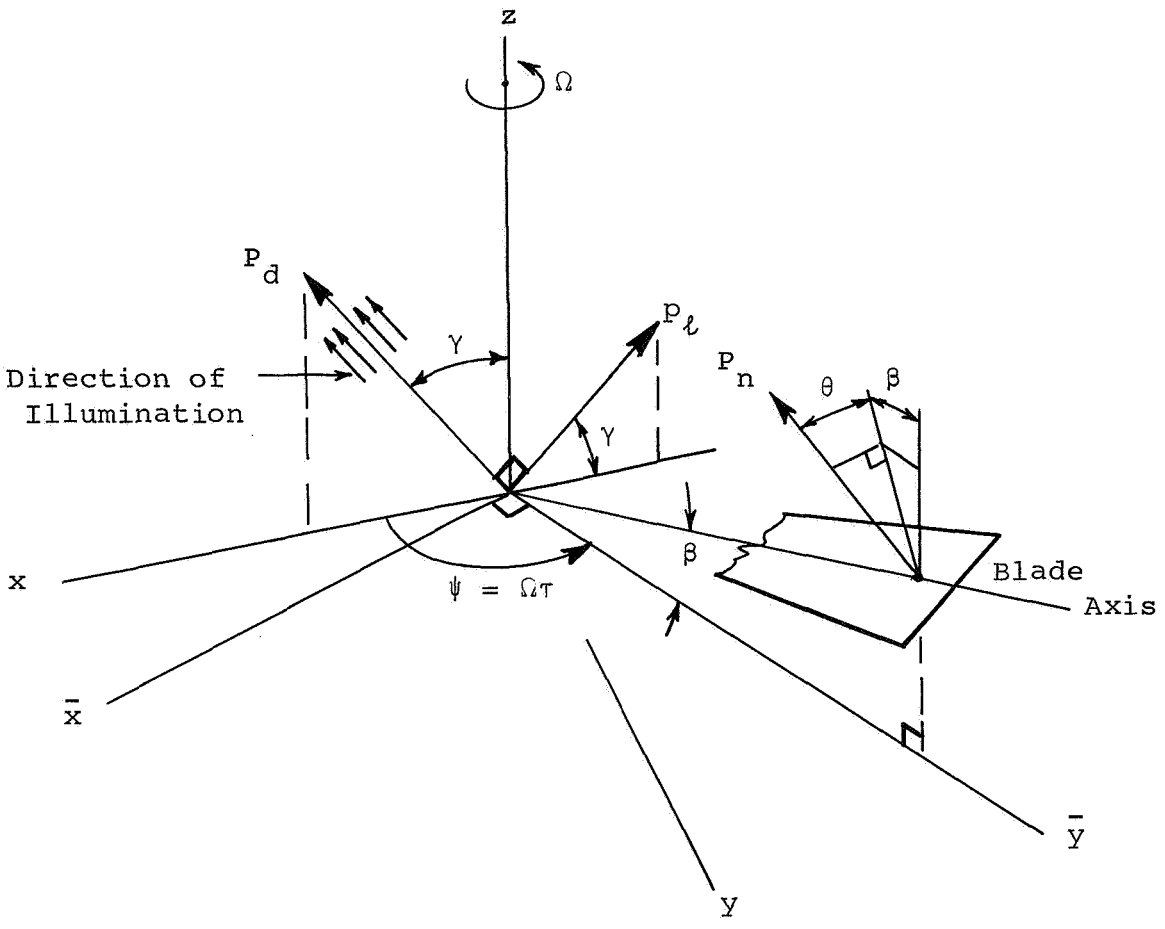

Figure 10. Coordinate Geometry For Rotating Blade

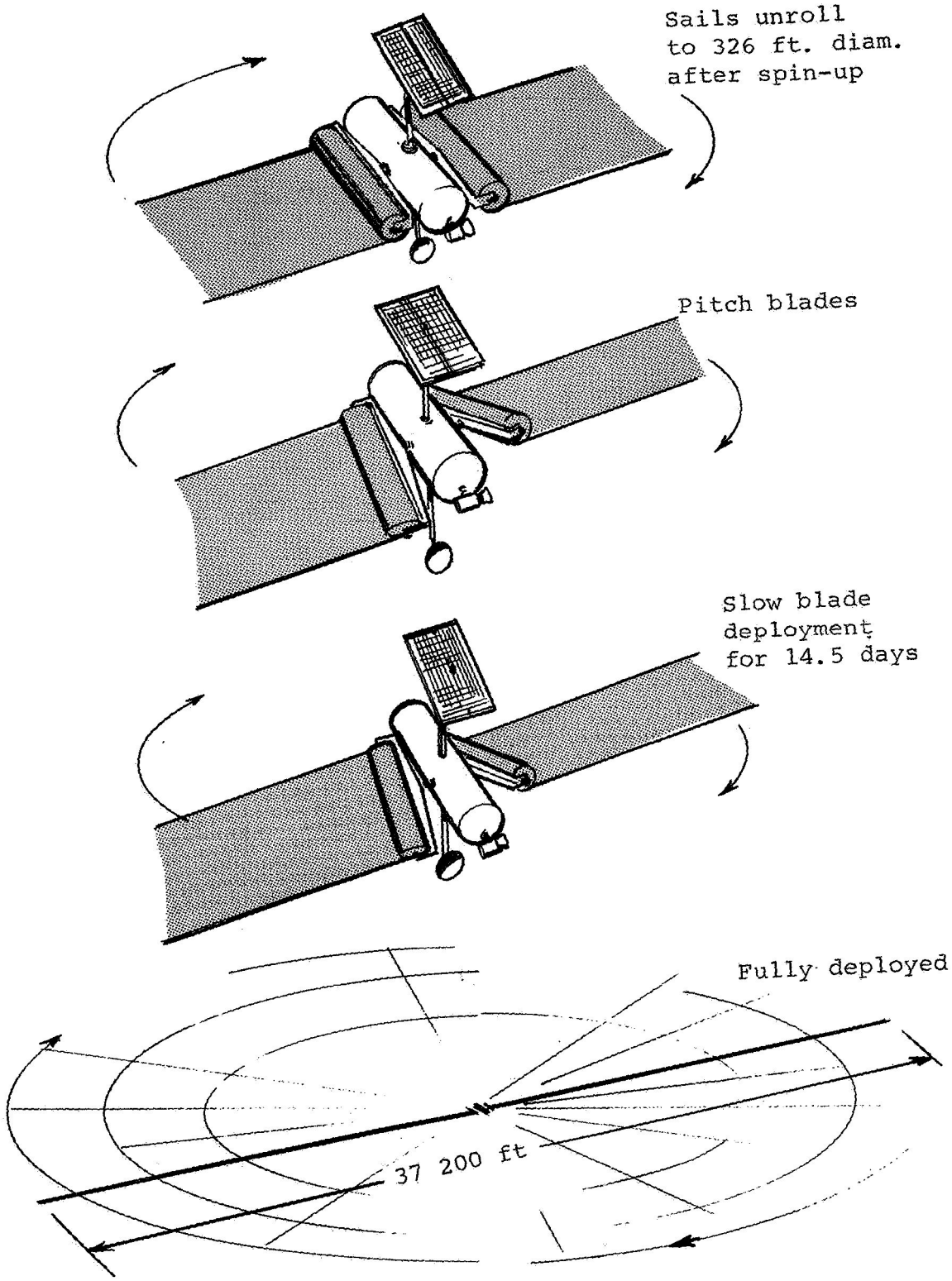

Figure 11. Deployment Sequence

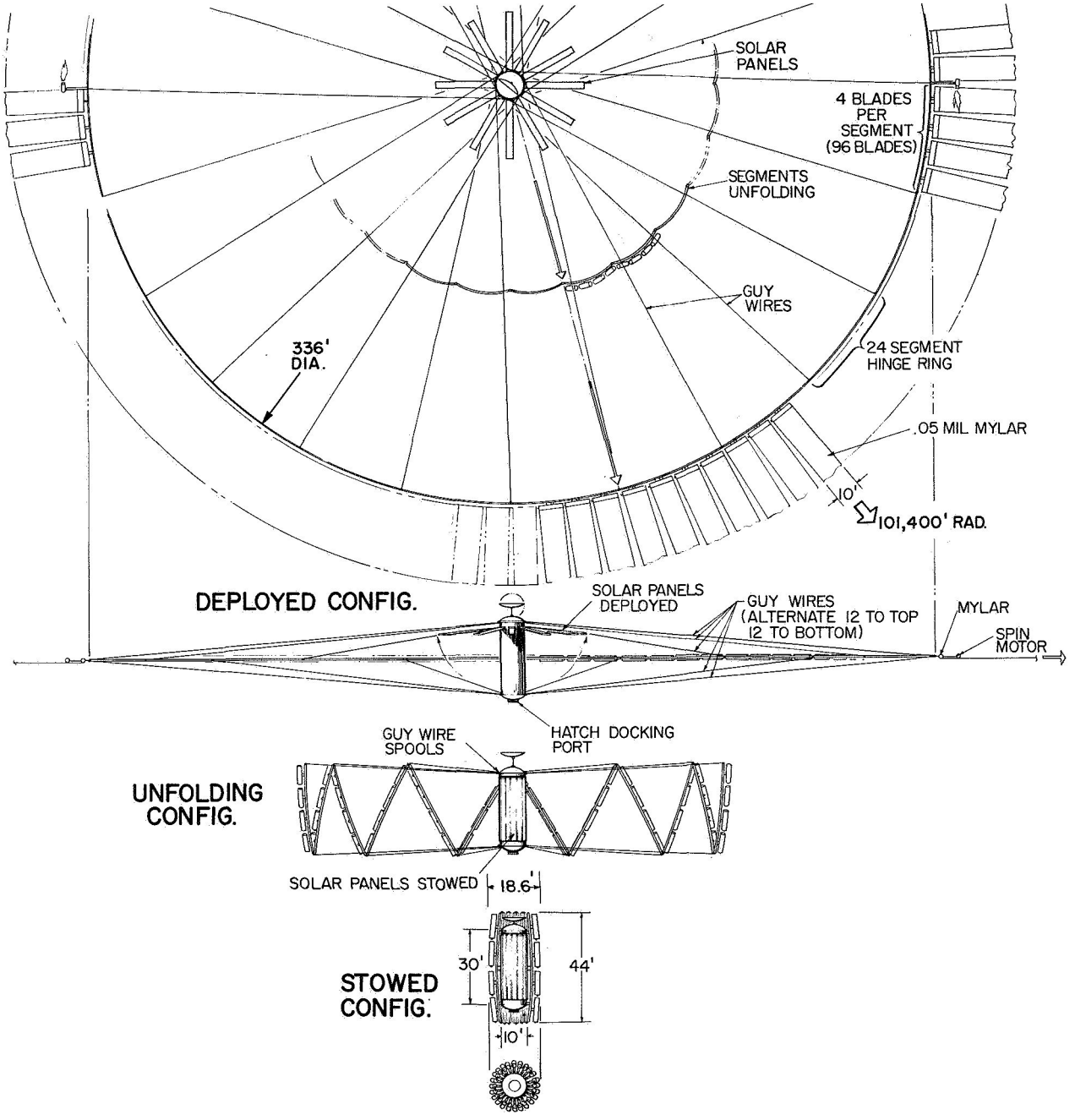

Figure 12. Pinwheel Heliogyro

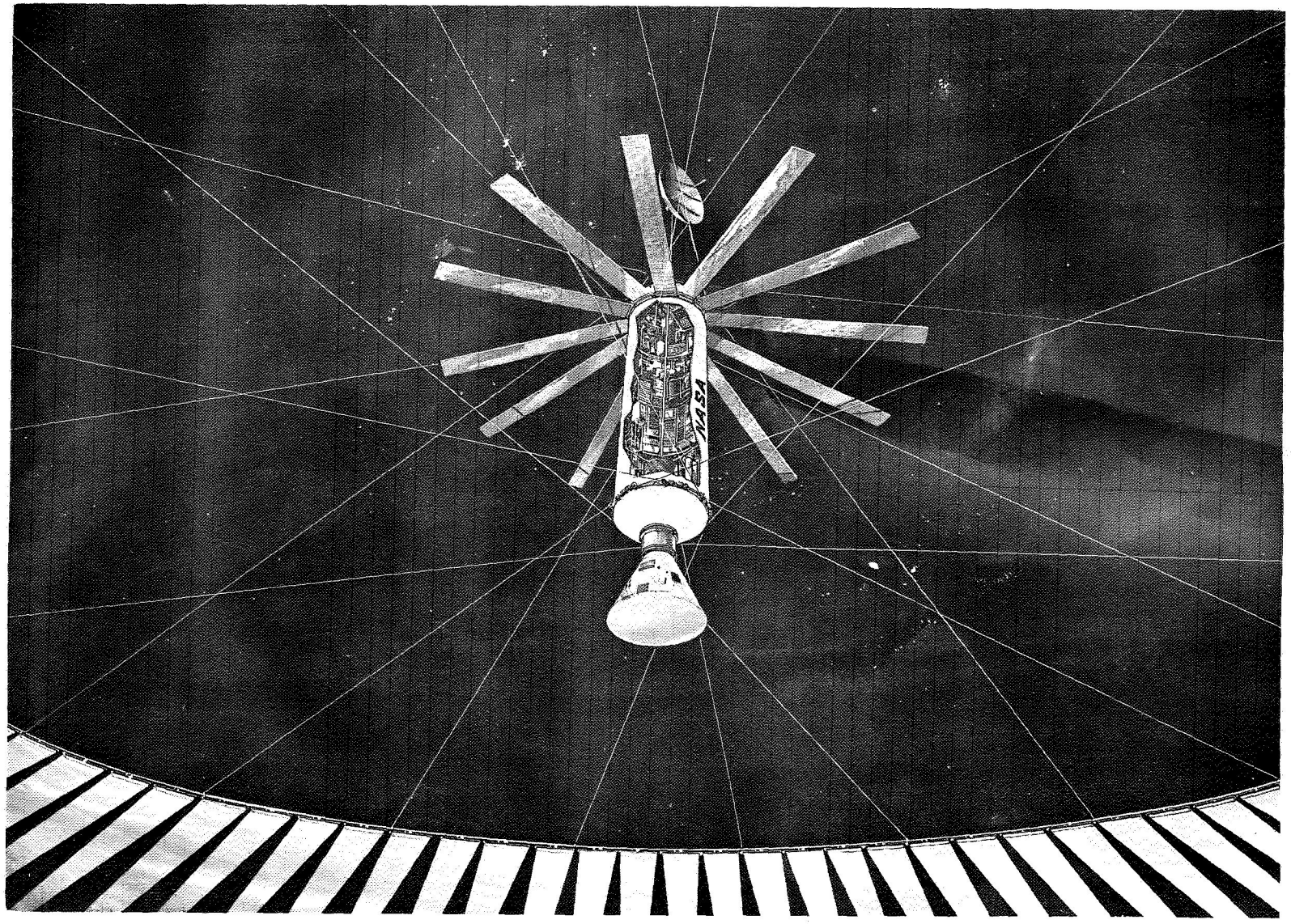

Figure 13. Artist's Concept of Pinwheel Heliogyro

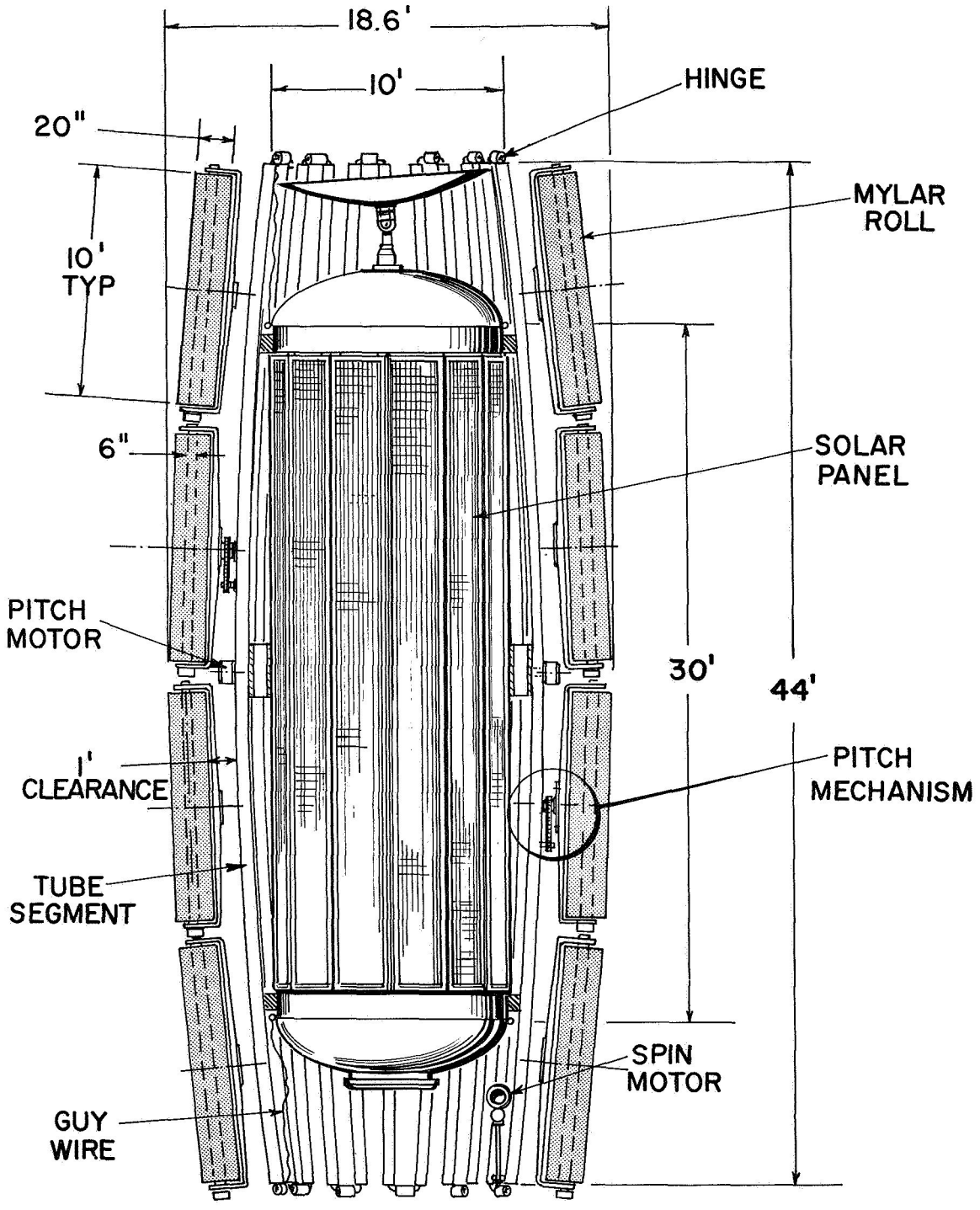

Figure 14. Pinwheel Heliogyro in Stowed Configuration

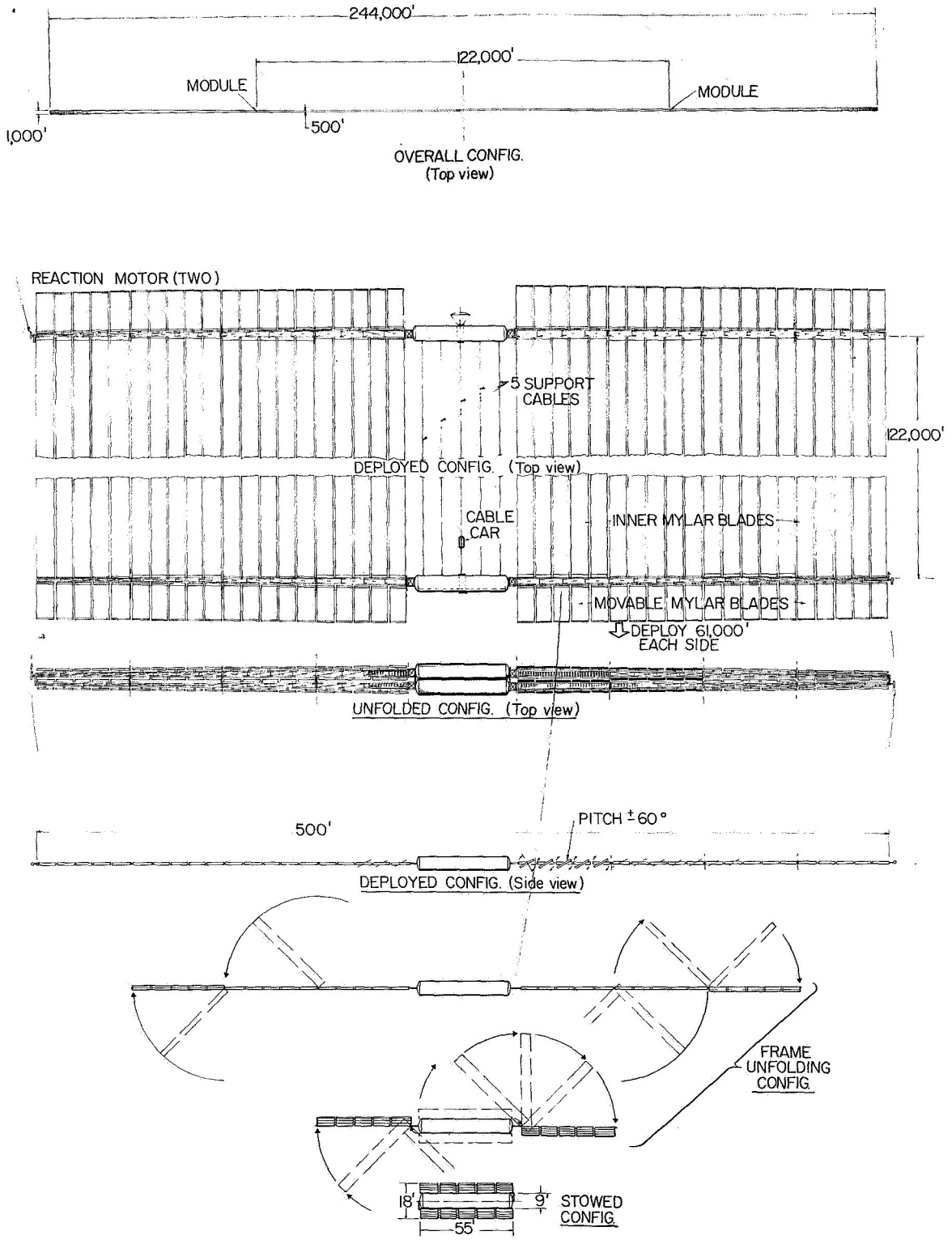

Figure 15. Parallel Blade Heliogyro

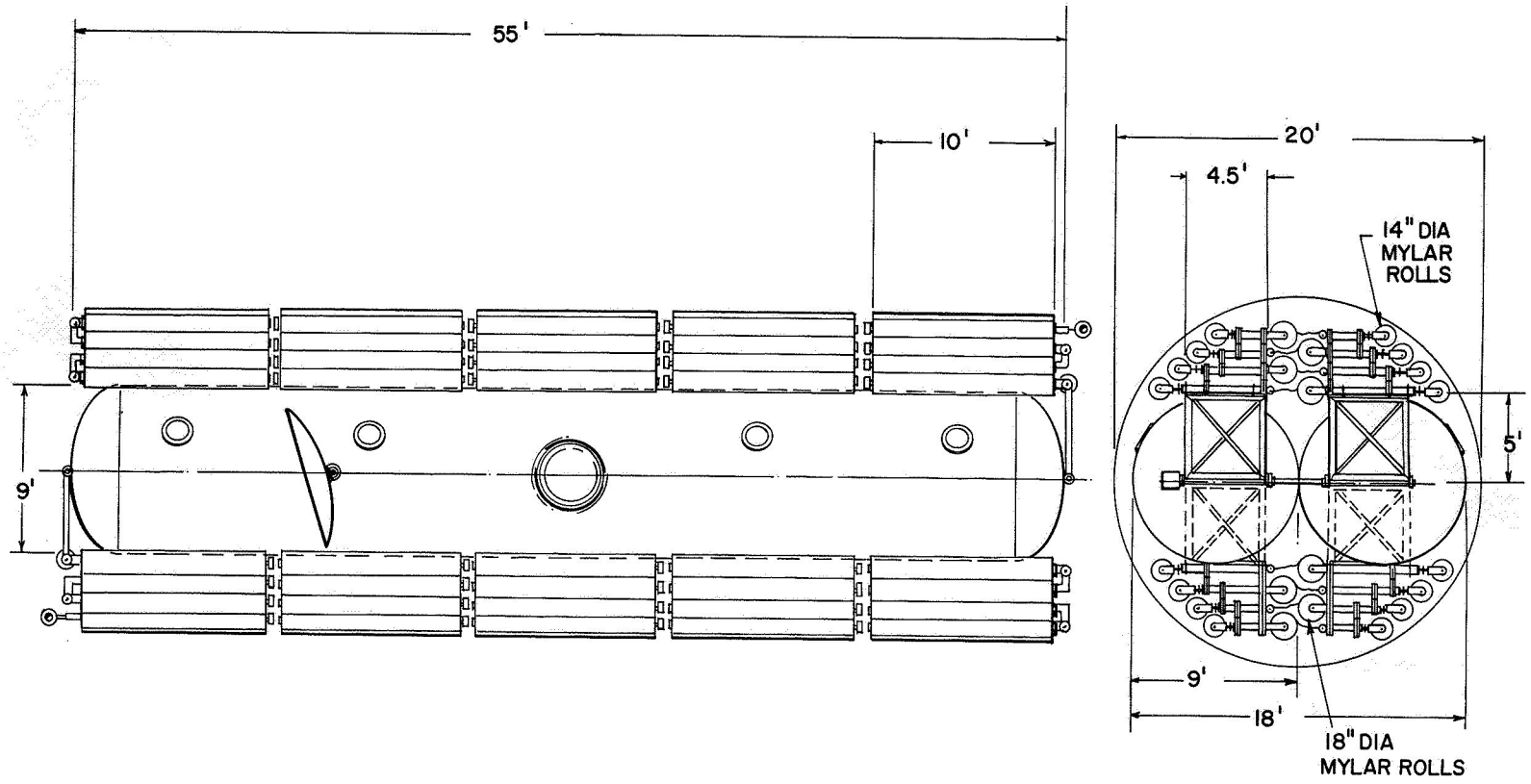

Figure 16. Parallel Blade Heliogyro in Stowed Configuration

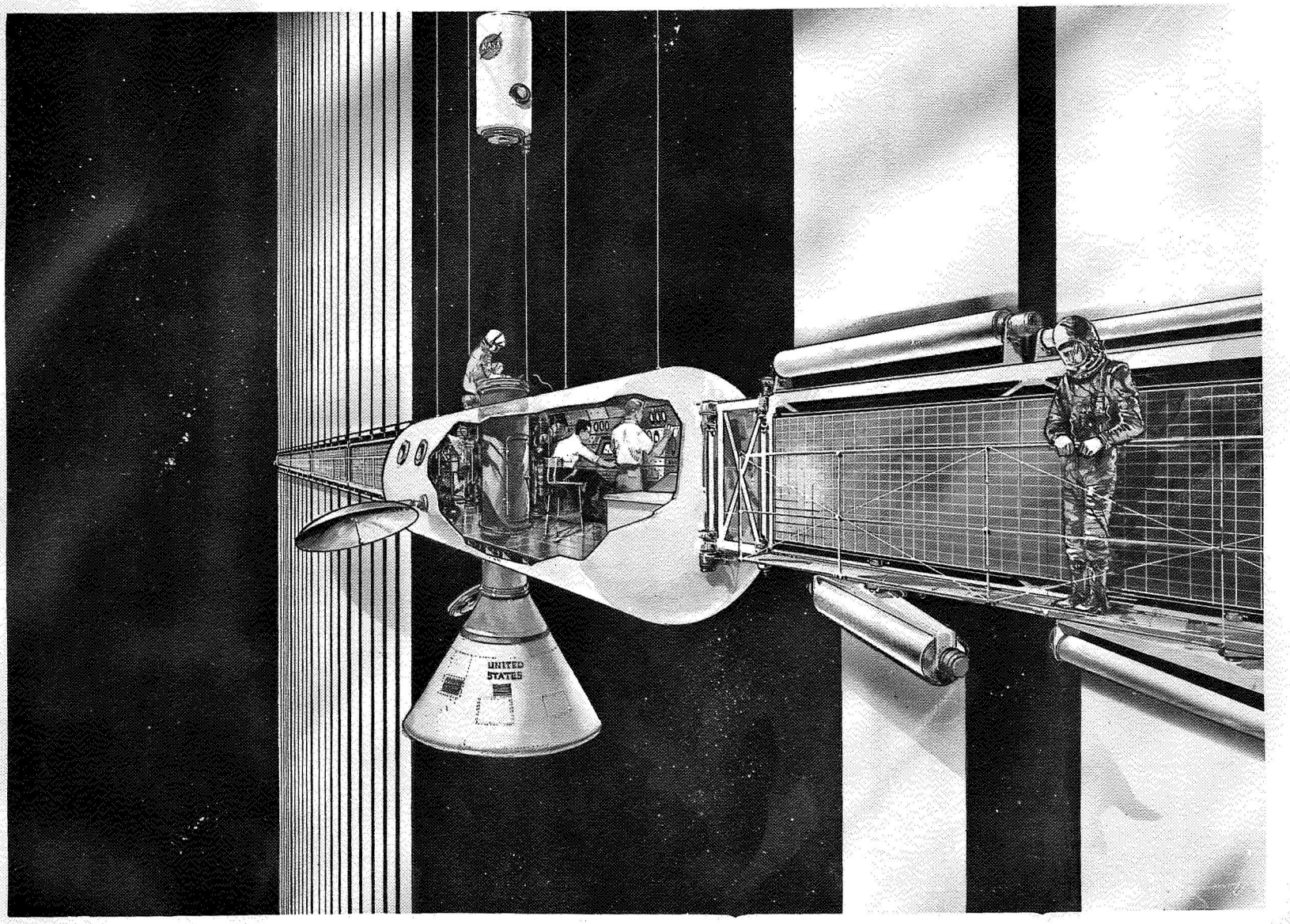

Figure 17. View of Payload Capsule

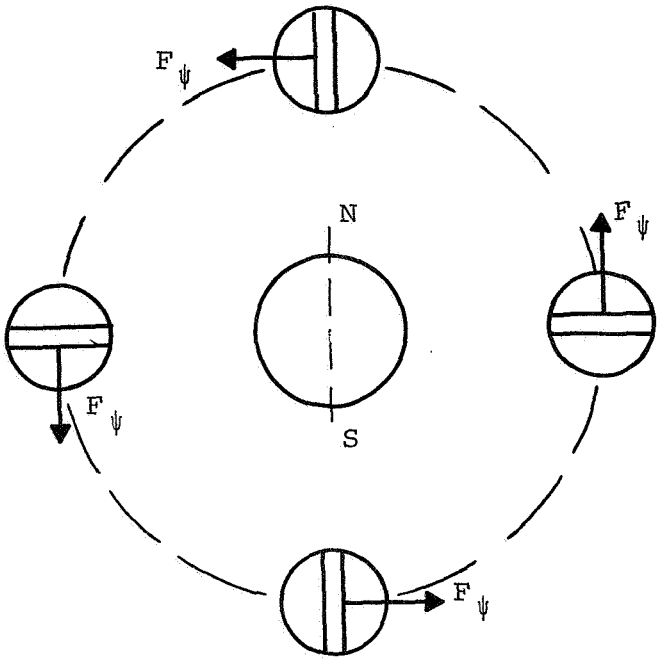

(a) Polar Orbit. Use Cyclic Pitch to Produce Lateral Force

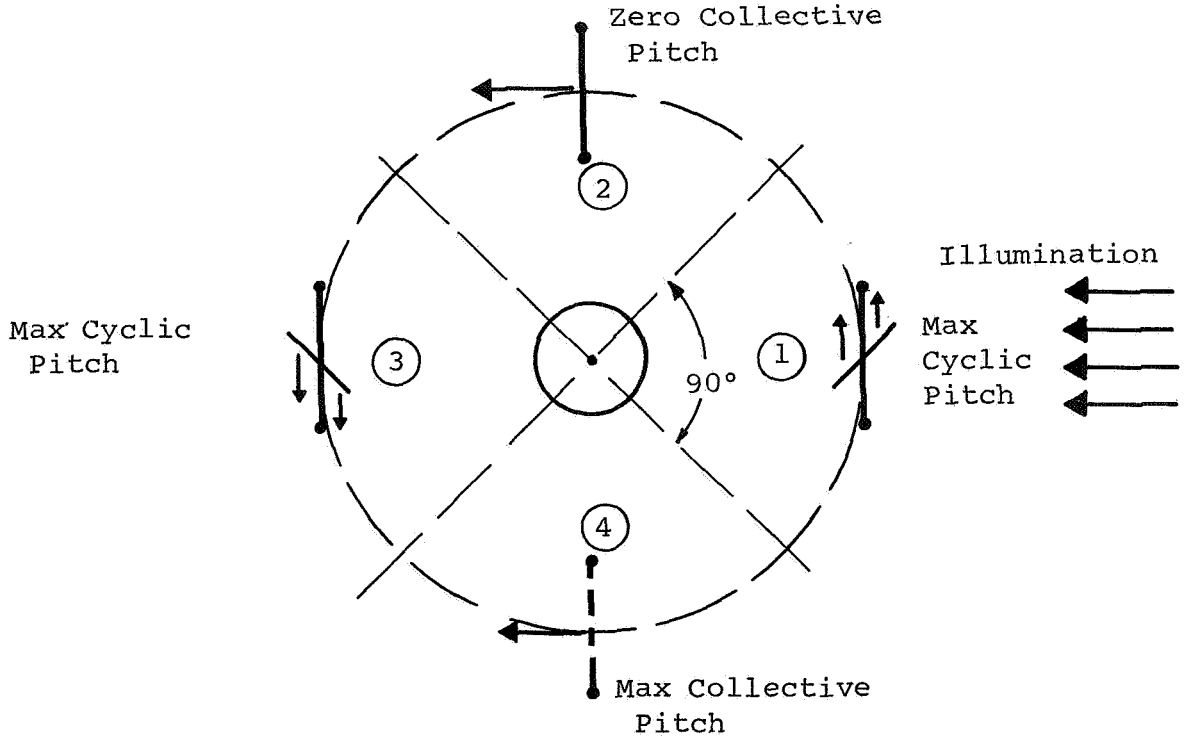

(b) Equatorial Orbit. Use Both Cyclic and Collective Pitch

Figure 18. Planetary Escape Maneuvers

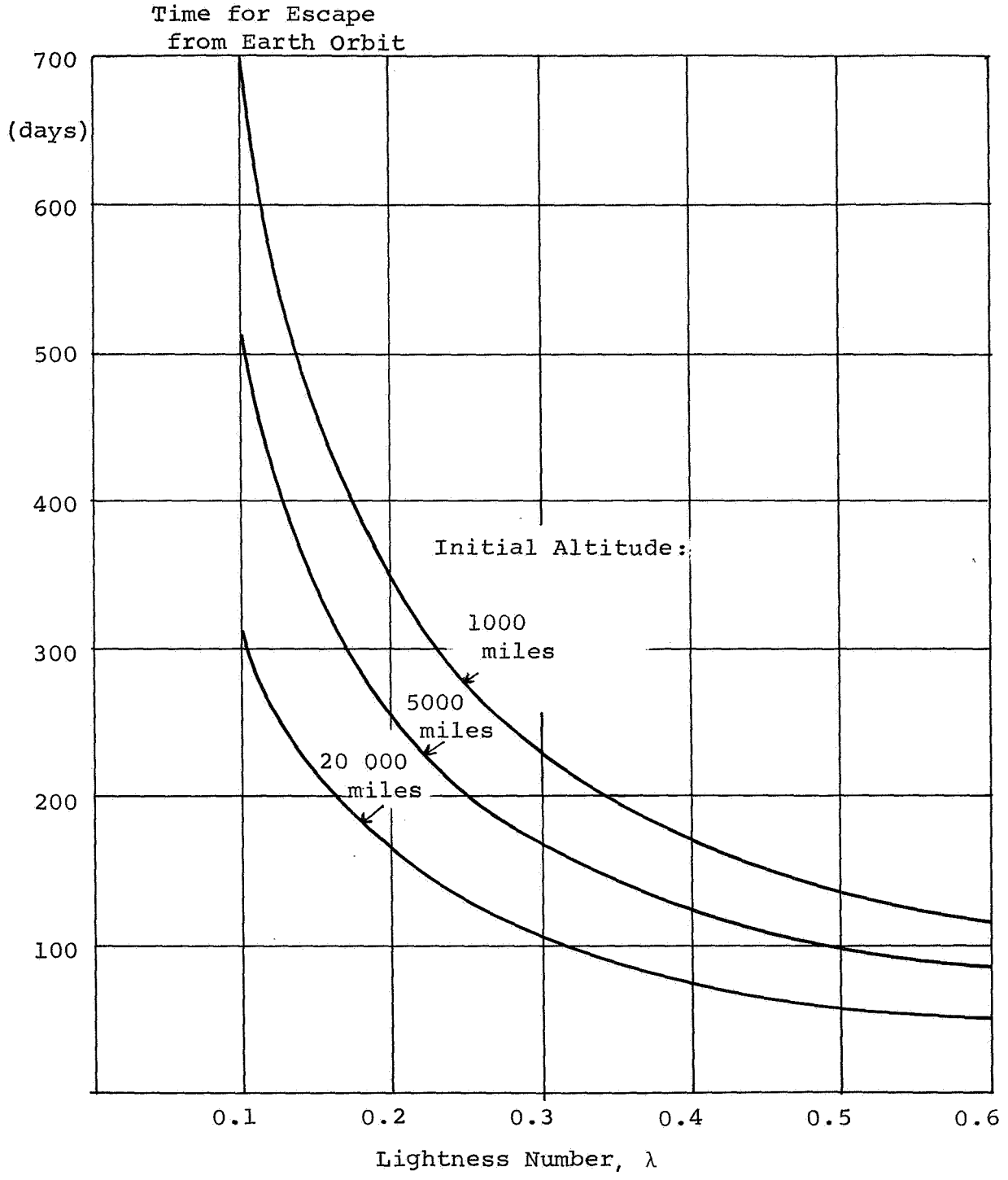

Figure 19. Time Required for Planetary Escape Maneuver from Earth Orbit

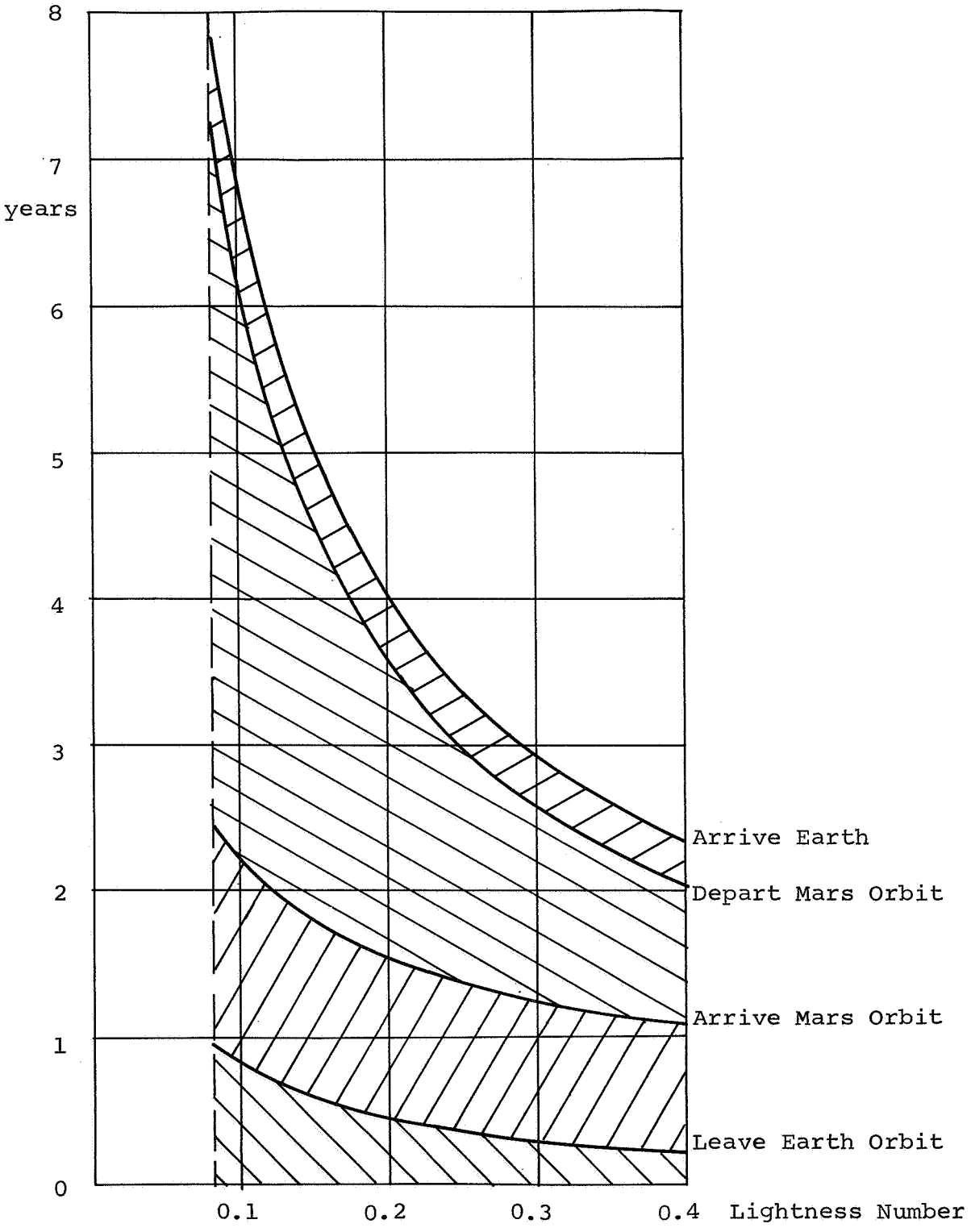

Figure 20. Elapsed Time for Mars Mission

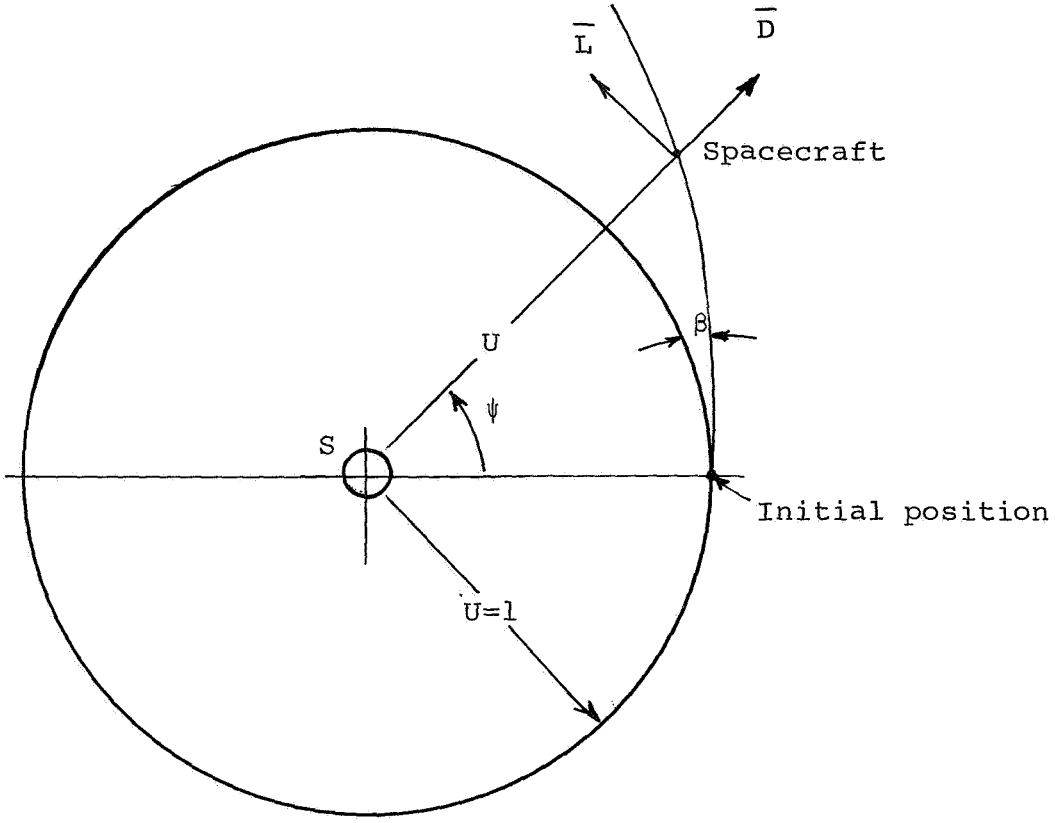

a) Coordinates and forces

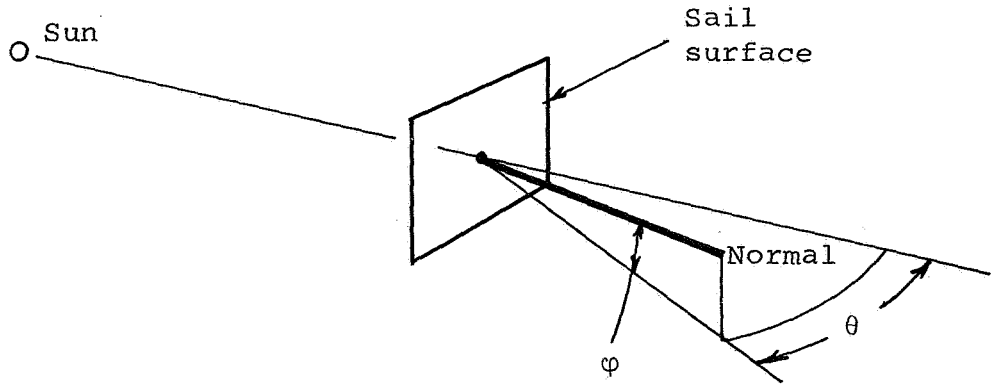

b) Local sail angles

Figure 21. Geometry of Flight

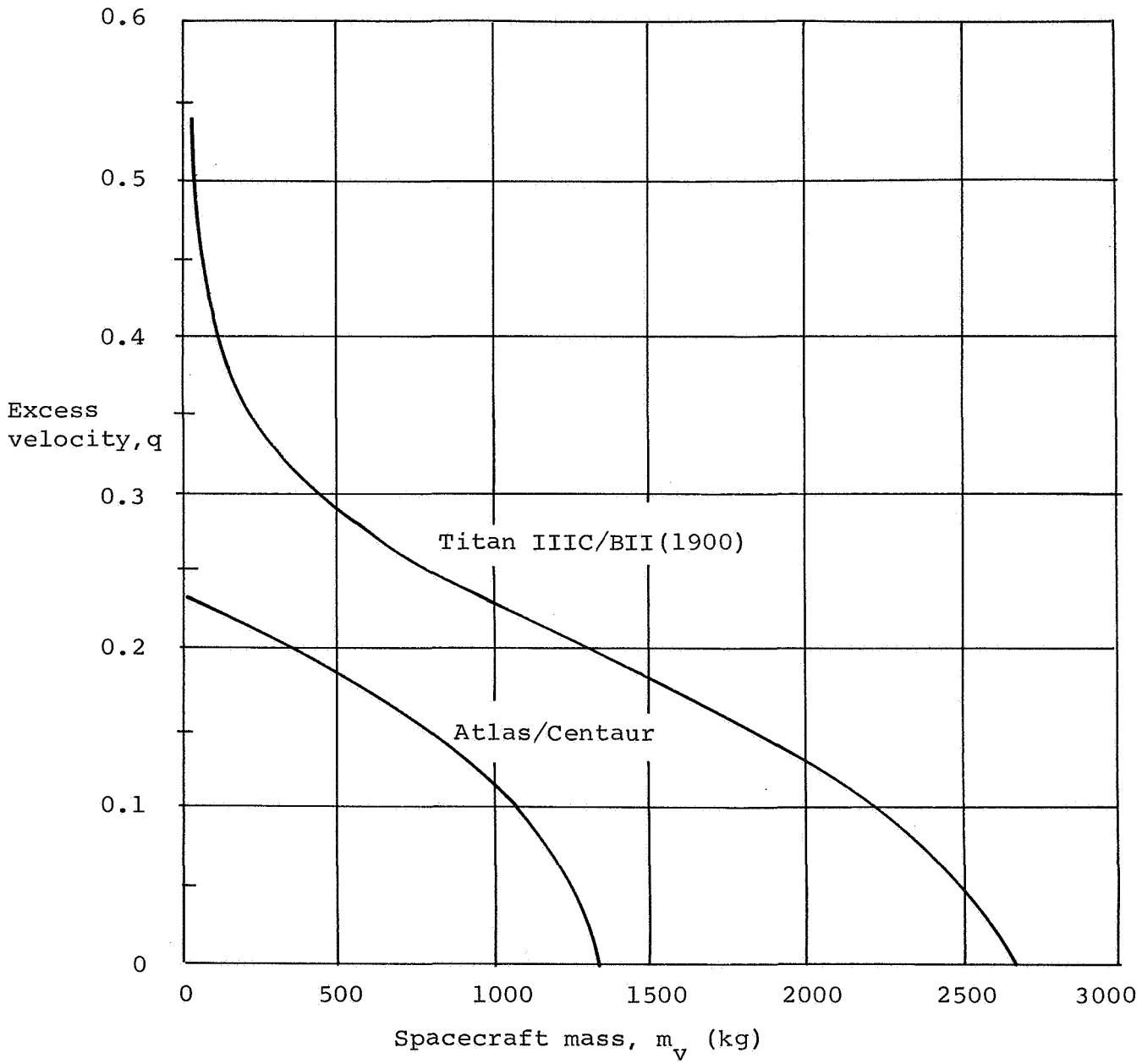

Figure 22. Variation in Excess Velocity with Payload Mass (Velocity measured in units of mean earth velocity around the sun)

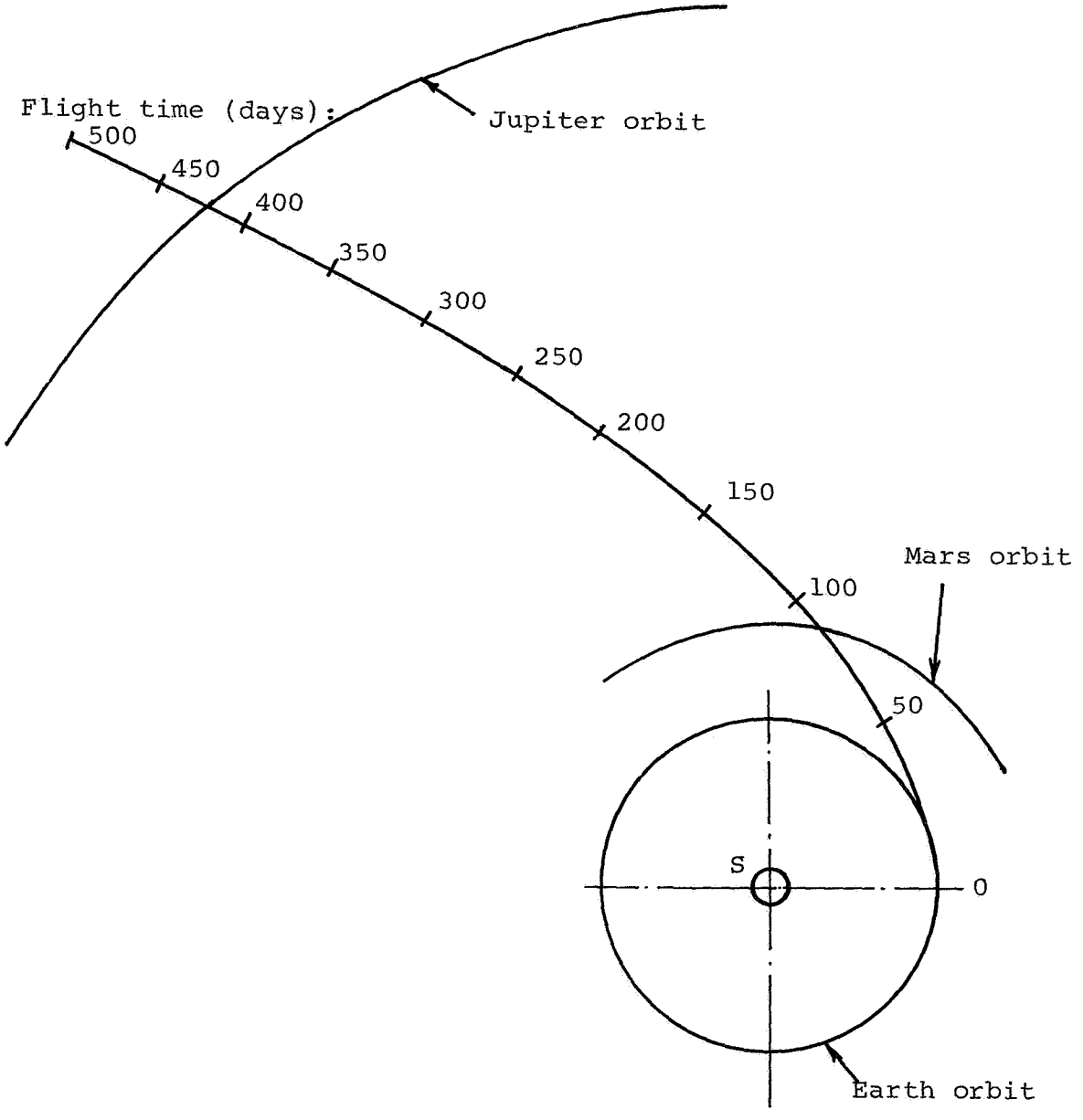

Figure 23. Sample Trajectory
(λ = 0.26, β = 0, q = 0.2)

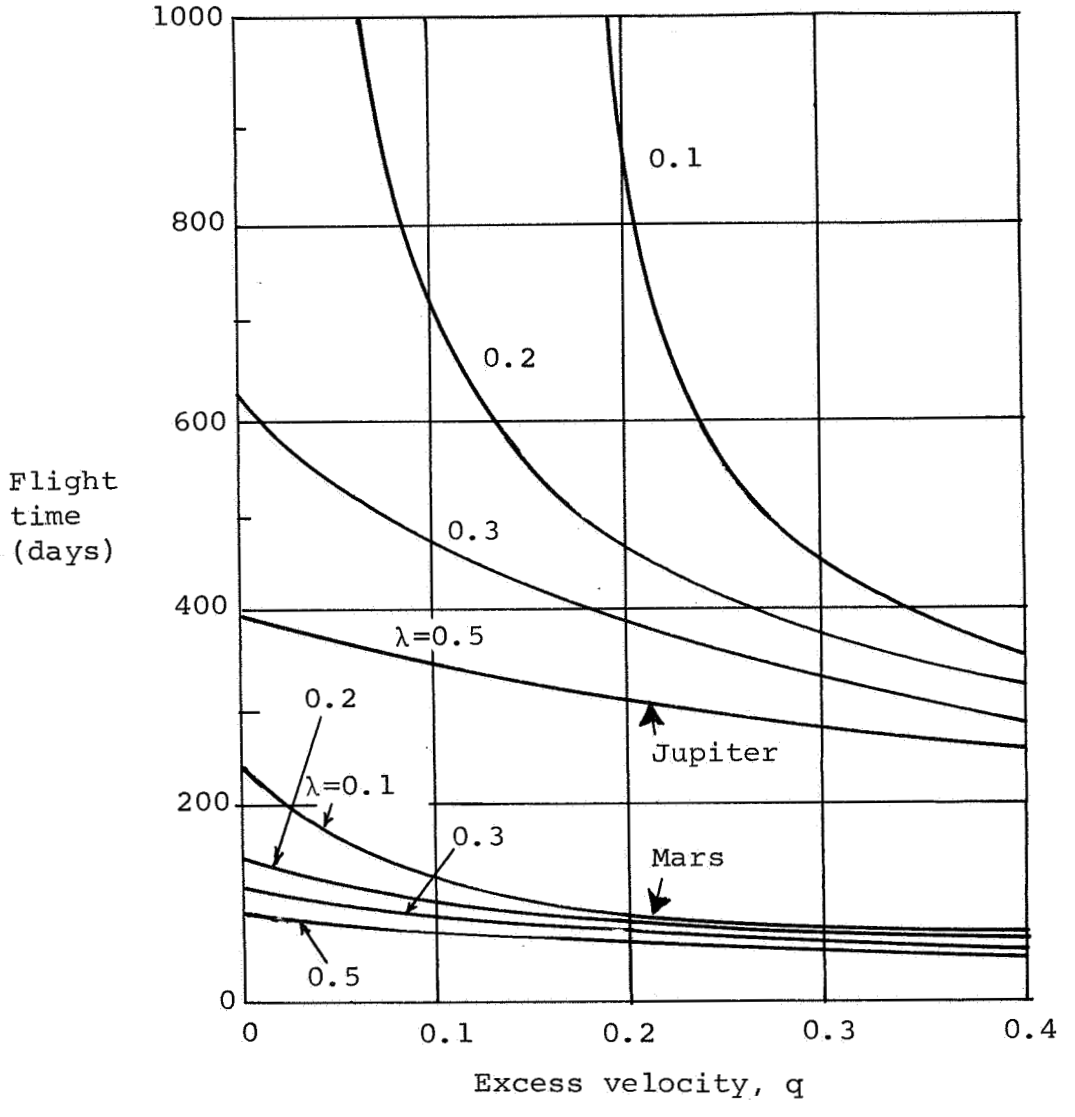

Figure 24. Basic Mission Results

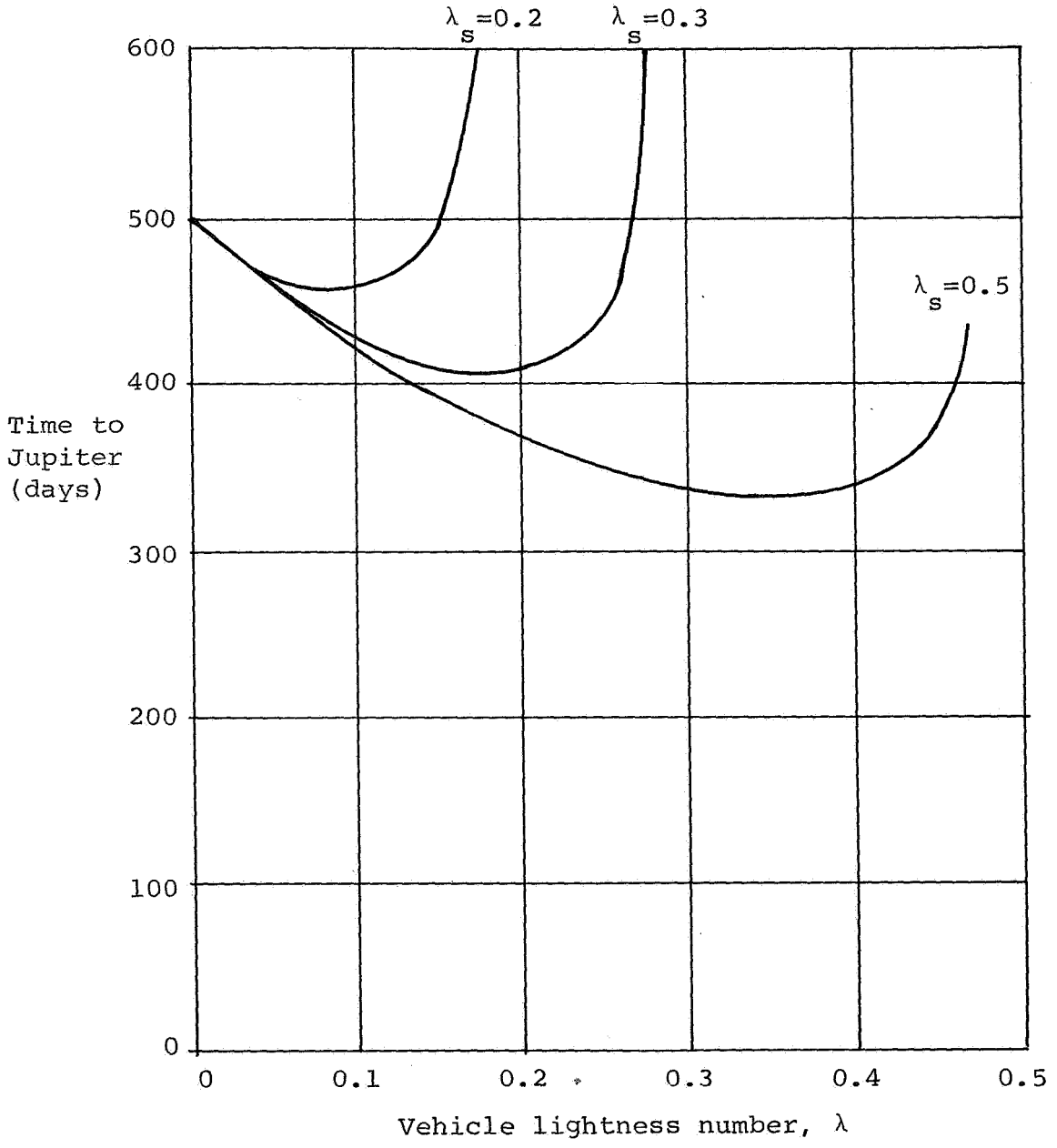

Figure 25. Variation in Flight Time with Vehicle Lightness Number for 227 kg Payload Mass and Fixed Sail Lightness Numbers

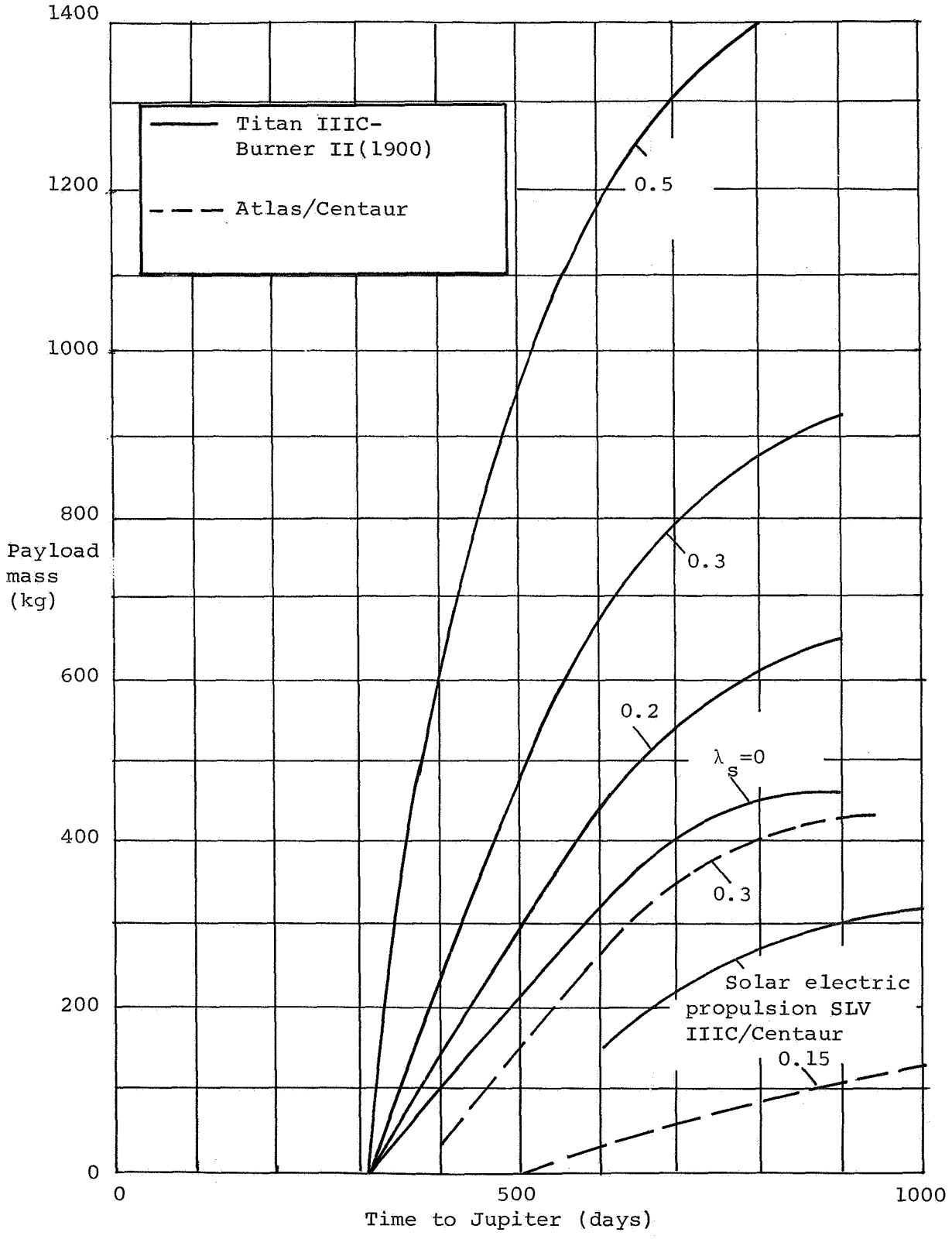

Figure 26. Jupiter Flyby Heliogyro Mission Parameters

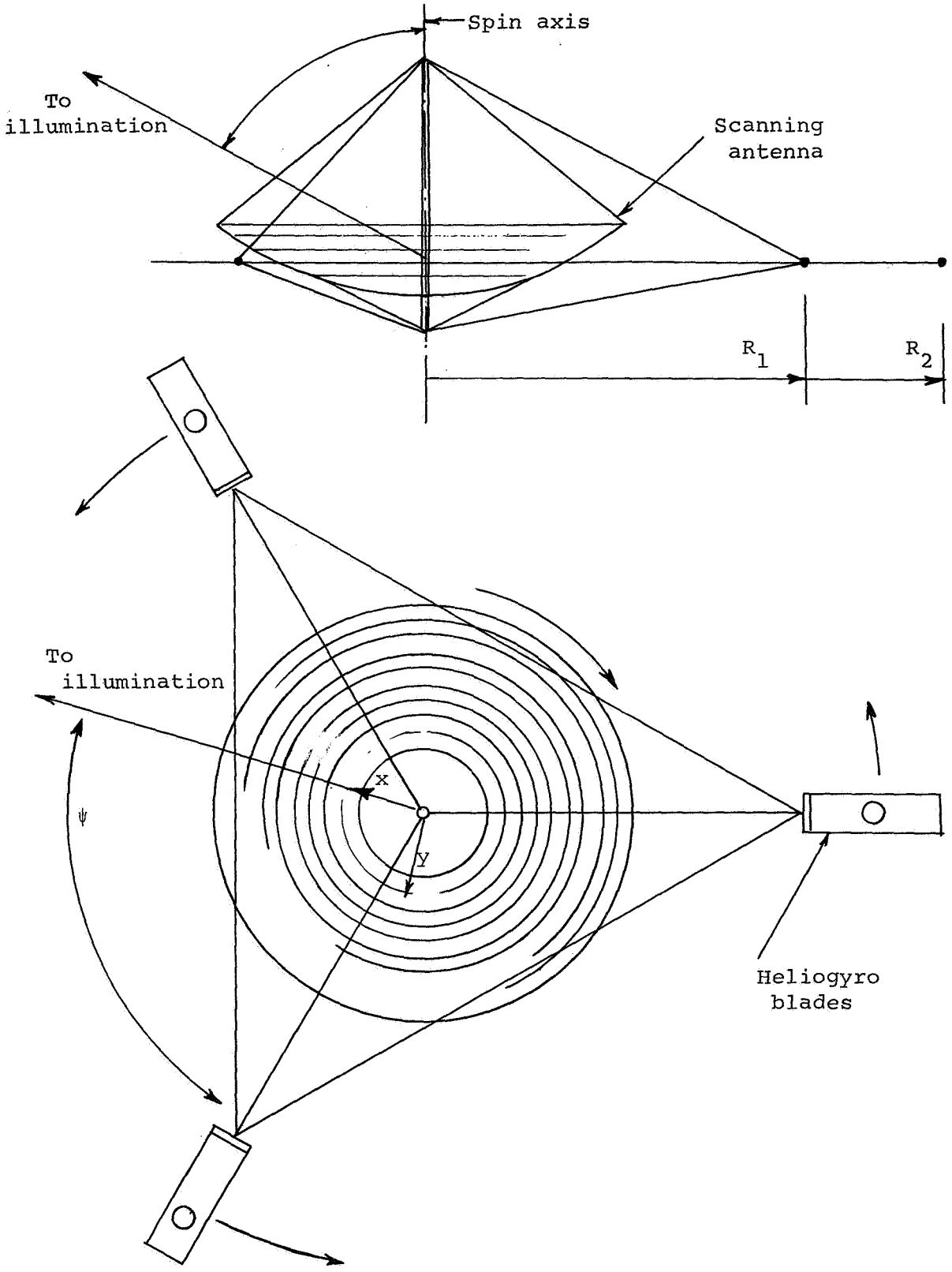

Figure 27. Attitude Control by Means of Heliogyro

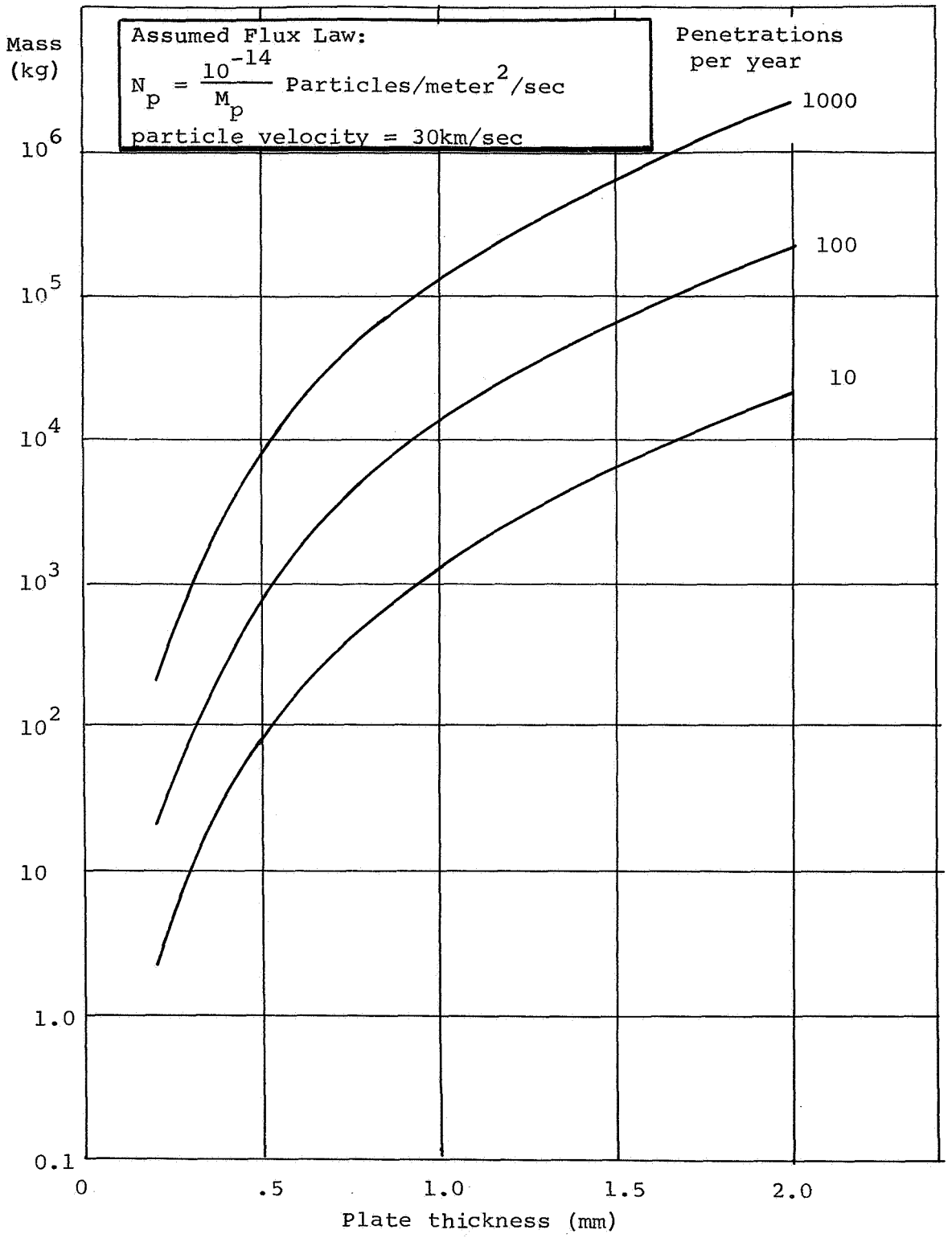

Figure 28. Mass of Steel Plate Required for Micrometeoroid Experiment

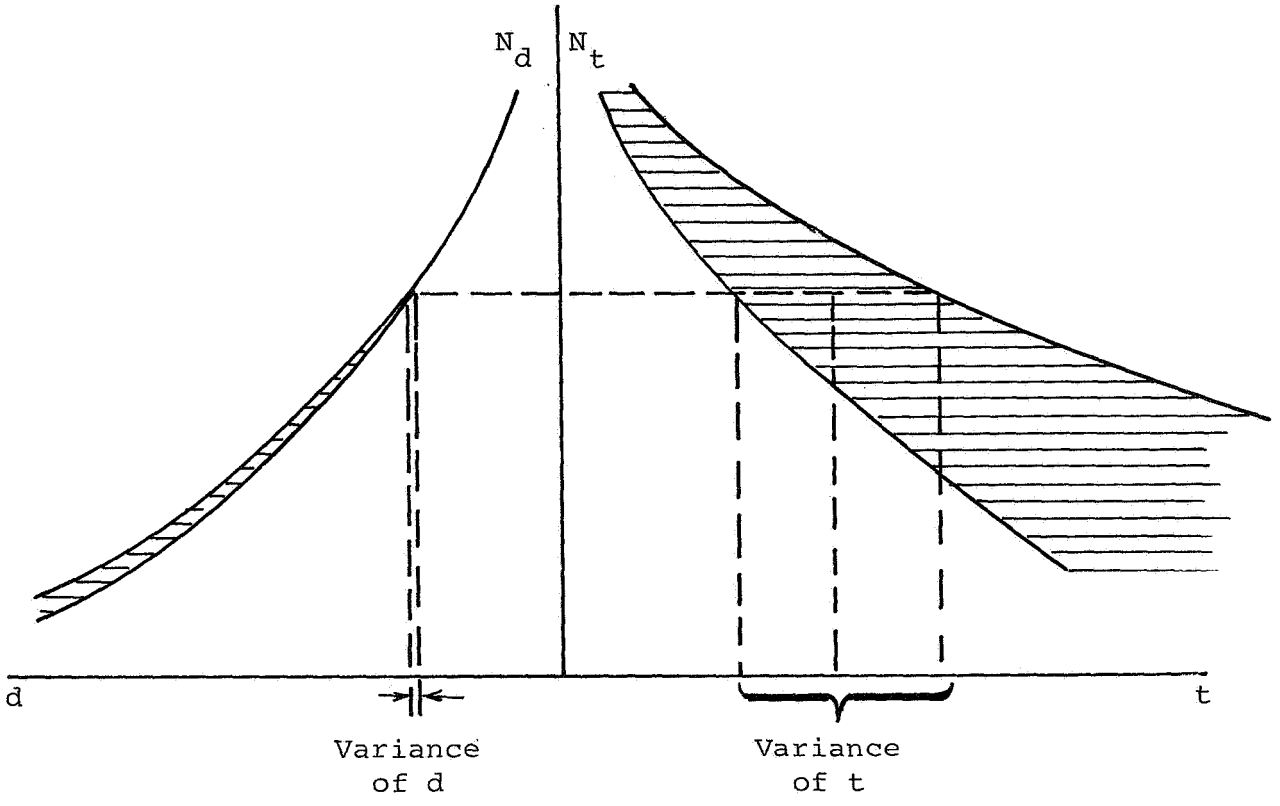

Figure 29. Flux Rate Variation with Diameter and Thickness

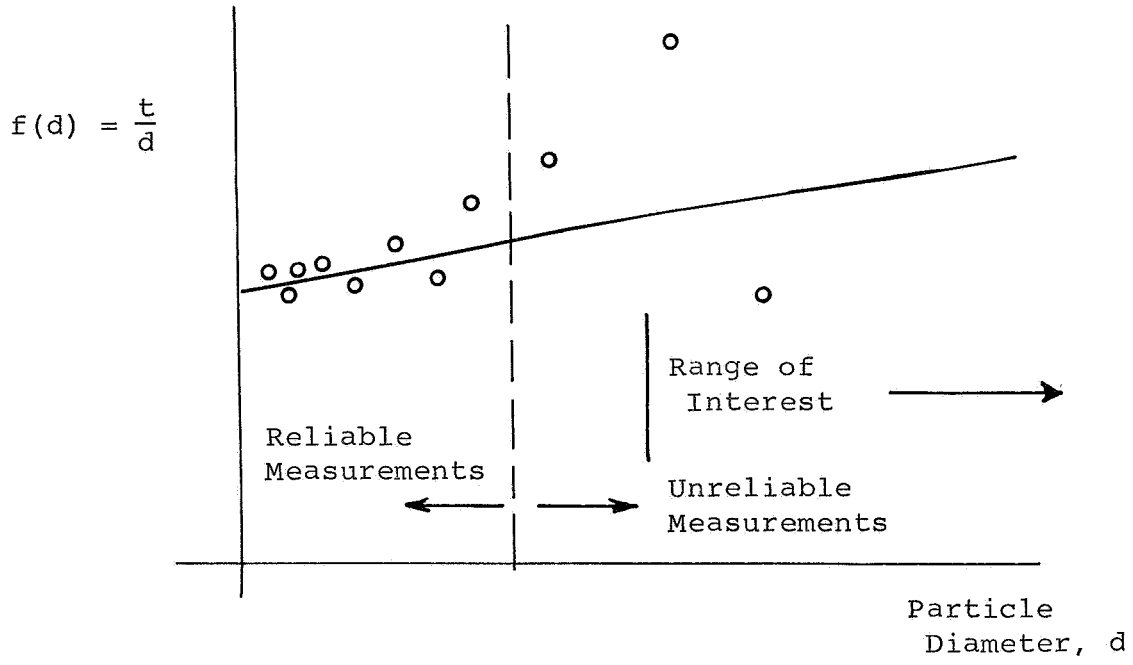

Figure 30. Assumed Variation of Particle Diameter Penetration Thickness

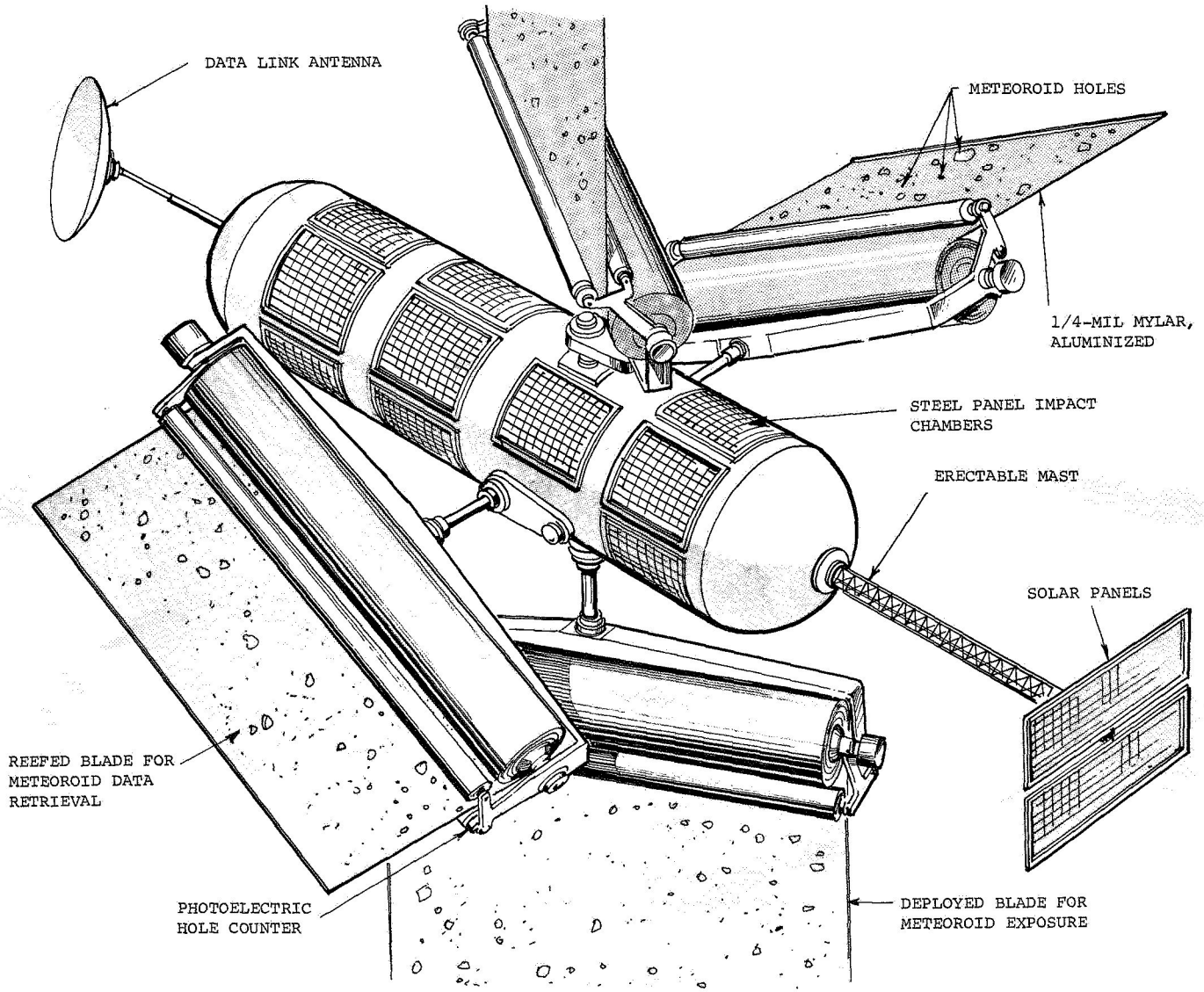

Figure 31. Heliogyro Meteoroid Surveyor

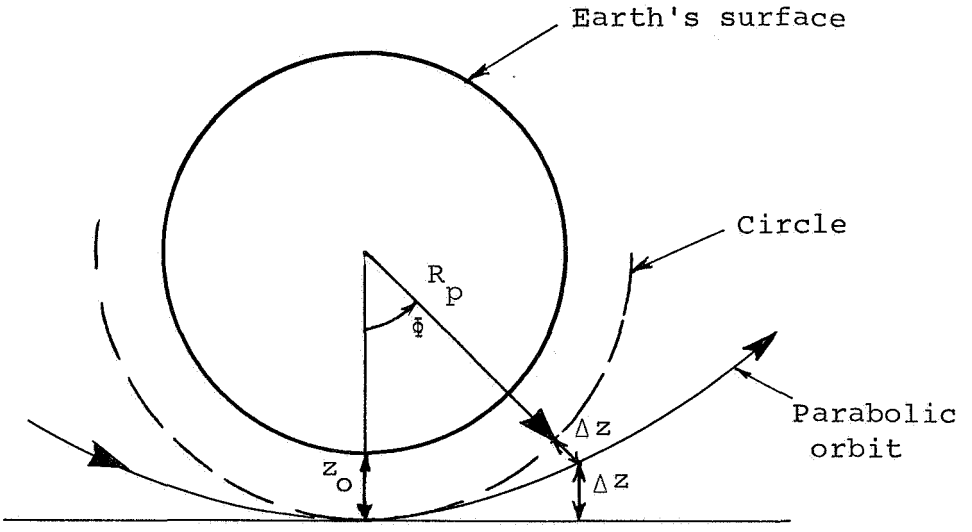

Figure 32. Geometrical Relationships for a Grazing Encounter

REFERENCES

1. Wiley, C. (pseudonym: Saunders, R.) "Clipper Ships of Space", Astounding Science Fiction, May 1951, p. 135.

2. Cotter, T. "Solar Sailing", Sandia Corporation Research Colloquium SCR-78, April 1959, Office of Technical Services, Dept. of Commerce, Washington, D.C.

3. Garwin, "Solar Sailing, a Practical Method of Propulsion within the Solar System", Jet Propulsion, March 1958.

4. Tsu, T., "Interplanetary Travel by Solar Sails", ARS Journal, June 1959.

5. Villers, P. "On the Application of Solar Radiation Momentum Transfer to Space Vehicle Propulsion", M.S. Thesis, Mass. Inst. of Tech., January 1960.

6. Gordon, B.J., "A Study of Interplanetary Travel by Solar Sail", M.S. Thesis, Air University, USAF, Wright-Patterson Air Force Base, Ohio, August 1961.

7. MacNeal, R.H., "The Heliogyro - An Interplanetary Flying Machine", Astro Research Corporation ARC-R-249, March 1967.

8. Kelley, H.J., "Gradient Theory of Optimal Flight Paths", ARS Journal, Vol. 30, p. 947-954, October 1960.

9. Wehner, G.K., Kenknight, C., and Rosenberg, D.L., "Sputtering Rates under Solar-Wind Bombardment", Planetary Space Science, Vol. 11, pp 885-895, 1963.

10. Hedgepeth, J.M., and Benton, M.D., "Analysis of Planetary Flyby Using the Heliogyro Solar Sailer", Astro Research Corporation ARC R-296, August 1968.

11. Schuerch, H.U., and Hedgepeth, J.M., "Large Low-Frequency Orbiting Radio Telescope", National Aeronautics and Space Administration, NASA CR-1201, October 1968.

12. MacNeal, R.H., "Meteoroid Damage to Filamentary Structures", Astro Research Corporation ARC-R-222, September 1966.

13. Sauer, C.G., "Trajectory Analysis and Optimization of a Low-Thrust Solar Electric Jupiter Flyby Mission", AIAA Paper 67-710, September 1967.

NASA-Langley, 1969 —— 31 CR-1329

NATIONAL AERONAUTICS AND SPACE ADMINISTRATION
WASHINGTON, D.C. 20546

OFFICIAL BUSINESS

FIRST CLASS MAIL

POSTAGE AND FEES PAID
NATIONAL AERONAUTICS A
SPACE ADMINISTRATION

POSTMASTER: If Undeliverable (Section 158
Postal Manual) Do Not Return

"The aeronautical and space activities of the United States shall be conducted so as to contribute . . . to the expansion of human knowledge of phenomena in the atmosphere and space. The Administration shall provide for the widest practicable and appropriate dissemination of information concerning its activities and the results thereof."

—NATIONAL AERONAUTICS AND SPACE ACT OF 1958

NASA SCIENTIFIC AND TECHNICAL PUBLICATIONS

TECHNICAL REPORTS: Scientific and technical information considered important, complete, and a lasting contribution to existing knowledge.

TECHNICAL NOTES: Information less broad in scope but nevertheless of importance as a contribution to existing knowledge.

TECHNICAL MEMORANDUMS: Information receiving limited distribution because of preliminary data, security classification, or other reasons.

CONTRACTOR REPORTS: Scientific and technical information generated under a NASA contract or grant and considered an important contribution to existing knowledge.

TECHNICAL TRANSLATIONS: Information published in a foreign language considered to merit NASA distribution in English.

SPECIAL PUBLICATIONS: Information derived from or of value to NASA activities. Publications include conference proceedings, monographs, data compilations, handbooks, sourcebooks, and special bibliographies.

TECHNOLOGY UTILIZATION PUBLICATIONS: Information on technology used by NASA that may be of particular interest in commercial and other non-aerospace applications. Publications include Tech Briefs, Technology Utilization Reports and Notes, and Technology Surveys.

Details on the availability of these publications may be obtained from:

SCIENTIFIC AND TECHNICAL INFORMATION DIVISION

NATIONAL AERONAUTICS AND SPACE ADMINISTRATION

Washington, D.C. 20546